UNCLASSIFIED
SECURITY CLASSIFICATION OF THIS PAGE

AD-A206 145

DTIC ELECTE MAR 1 1989

REPORT DOCUMENTATION PAGE

1b. RESTRICTIVE MARKINGS	
2a. SECURITY CLASSIFICATION AUTHORITY	3. DISTRIBUTION / AVAILABILITY OF REPORT: APPROVED FOR PUBLIC RELEASE DISTRIBUTION IS UNLIMITED
2b. DECLASSIFICATION / DOWNGRADING SCHEDULE	
4. PERFORMING ORGANIZATION REPORT NUMBER(S)	5. MONITORING ORGANIZATION REPORT NUMBER(S): AFOSR-TR- 89-0287
6a. NAME OF PERFORMING ORGANIZATION: Iowa State University	6b. OFFICE SYMBOL (If applicable): NA
7a. NAME OF MONITORING ORGANIZATION: AFOSR/NA	
6c. ADDRESS (City, State, and ZIP Code): Dept. of Aerospace Engineering, Ames, IA 50011	7b. ADDRESS (City, State, and ZIP Code): BUILDING 410, BOLLING AFB, DC 20332-6448
8a. NAME OF FUNDING / SPONSORING ORGANIZATION: AFOSR	8b. OFFICE SYMBOL (If applicable): NA
9. PROCUREMENT INSTRUMENT IDENTIFICATION NUMBER: AFOSR Grant 85-0357	
8c. ADDRESS (City, State, and ZIP Code): BUILDING 410, BOLLING AFB, DC 20332-6448	10. SOURCE OF FUNDING NUMBERS: PROGRAM ELEMENT NO. 61102F; PROJECT NO. 2307; TASK NO. A1; WORK UNIT ACCESSION

11. TITLE (Include Security Classification)

"Three Dimensional High Speed Boundary Layer Flows"

12. PERSONAL AUTHOR(S)
George R. Inger

13a. TYPE OF REPORT	13b. TIME COVERED	14. DATE OF REPORT (Year, Month, Day)	15. PAGE COUNT
Final Technical Rpt	FROM SEP 85 TO MAY 88	September 28, 1988	44

16. SUPPLEMENTARY NOTATION

17. COSATI CODES			18. SUBJECT TERMS (Continue on reverse if necessary and identify by block number)
FIELD	GROUP	SUB-GROUP	Viscous-Inviscid Interactions High Speed Turbulent Boundary Layers Vortex Arrays

19. ABSTRACT (Continue on reverse if necessary and identify by block number)

This final report summarizes the research results obtained by a two-faceted basic theoretical investigation involving (1) fundamental analyses of three-dimensional viscous-inviscid interaction effects within high speed turbulent boundary layers and (2) study of the influence of streamwise vortex arrays on the skin friction within attached or separated laminar layer flows. The work described was carried out from September 1985 to May 31, 1988.

20. DISTRIBUTION / AVAILABILITY OF ABSTRACT	21. ABSTRACT SECURITY CLASSIFICATION
☐ UNCLASSIFIED/UNLIMITED ☒ SAME AS RPT ☐ DTIC USERS	UNCLASSIFIED

22a. NAME OF RESPONSIBLE INDIVIDUAL	22b. TELEPHONE (Include Area Code)	22c. OFFICE SYMBOL
LEN SAKELL	202-767-4935	AFOSR/NA

DD FORM 1473, 84 MAR — 83 APR edition may be used until exhausted. All other editions are obsolete.

SECURITY CLASSIFICATION OF THIS PAGE
UNCLASSIFIED

AFOSR GRANT 85-0357

"Three Dimensional High Speed Boundary Layer Flows"

FINAL TECHNICAL REPORT

G. R. Inger

Iowa State University

Ames, Iowa 50011

September 28, 1988

TABLE OF CONTENTS

ABSTRACT

This final report summarizes the research results obtained by a two-faceted basic theoretical investigation involving (1) fundamental analyses of three-dimensional viscous-inviscid interaction effects within high speed turbulent boundary layers and (2) study of the influence of streamwise vortex arrays on the skin friction within attached or separated laminar layer flows. The work described was carried out from September 1985 to May 31, 1988.

1. INTRODUCTION

The overall objective of this research was the basic theoretical investigation of three-dimensional pressure, skin friction, and flow field disturbances in both laminar and turbulent boundary layer flows including viscous-inviscid interaction effects, separation and reattachment. A sound understanding of these phenomena is required in modern aerodynamic design analyses of high-speed flight vehicles. Indeed, the interest in and need for such research appears to be even stronger now than when the current investigation was first begun.

Broadly speaking, the primary emphasis in our studies has been to seek a basic physical understanding of the underlying fluid behavior by means of analytically-oriented methods; in this way, the results can be used to guide and interpret concurrent experimental and computationally oriented investigations. Specifically, our inquiry has focused on two parallel paths of investigations: (1) three-dimensional viscous-inviscid interaction phenomena within turbulent boundary layers in supersonic flow due to impinging swept shock and/or 3-D surface deflections; and (2) streamwise vortex-disturbance mechanisms within boundary layers that are either separated or attached. The project has proven very successful both in solving a number of the target flow problems and in developing new ideas and tools; this report summarizes these results.

2. SUMMARY OF ACCOMPLISHMENTS

2.1. Studies of Boundary Layer Vortex Effects

A major phase of the streamwise vortex investigation culminated in applying our previously-developed theory[1-5] of disturbance vortex-pair formation in separating boundary layer flows to the analysis of streamwise vortex structure in the near wake of stalling wings operating at low Reynolds numbers (see Fig. 1). A paper on this work was presented to the Royal Aeronautical Society at its October 1986 meeting on Low Reynolds Number Aerodynamics in London and has been published in the Proceedings of the Meeting.[6]

A second achievement was the completion of a detailed analytical study of spanwise, periodic 3-D disturbances (representative of an array of counter-rotating pairs of streamwise vortices) within an entire family of host pressure-gradient laminar boundary layer flows, namely the self-similar incompressible Faulkner-Skan flows along a wedge (Figure 2). In addition to correcting and explaining several key features of Fannelop's earlier study of the flat plate limit of this problem,[7] our new results significantly extend the basic understanding of how streamwise vortices alter the flow, skin friction, and incipient separation behavior of nominally 2-D boundary layer flows. This work was documented by the M.S. thesis of Mr. M. Konno and has been submitted for publication (an abstract of this paper is included as Appendix A of this report).

The aforementioned work was subsequently extended to treat the situation where the streamwise vortices are generated at the wall by small spanwise ripples in its surface that grow linearly in amplitude in the downstram direction. The results were presented in a paper at the Summer 1986 U.S. National Fluid Mechanics Conference, a copy of which is attached as Appendix B.

2.2 Theoretical Investigation of Three-Dimensional Turbulent Interactions

This aspect of our research had three major goals:

- Apply modern asymptotic methods (high-Re) to elucidate the basic flow field physics of 3-D interactions, especially near the surface;
- Extract the fundamental similtude laws governing swept interactions within the framework of "Law of the Wall/Wake" concepts that characterize the incoming turbulent boundary layer;
- Assess the validity of the "Independence Principle" approximation for some representative compressible turbulent interactive flows.

In general support of these studies we first completed a basic theoretical study of nonisotropic turbulence model effects on the Law of the Wall region of nonseparating three-dimensional turbulent boundary layers (this work was subsequently factored into our analyses of swept shock/turbulent boundary layer interaction[8,9]). A paper on this work was prepared for the January 1987 AIAA Aerospace Sciences Meeting (Fig. 3).

Next, a major emphasis was placed in recent years on further refinement of our original swept-shock interaction theory[8] for cylindrically-symmetric flows (Fig. 4). Our approach is based on the 3-D extension of our previously successful nonasymptotic triple-deck interaction theory (Fig. 5), combined with the aforementioned nonisotropic 3-D viscosity model. A paper on the application of this theory to the swept compression ramp problem was presented in July 1985 to the AIAA 18th Fluid and Plasma Dynamics Conference[9] and subsequently in September 1985 to the IUTAM Symposium on Turbulent Shear Layer/Shock Wave Interactions held in Paris, being published in the proceedings of the latter.[10] Among the many new analytical results obtained were (a) relationships governing the generation of significant secondary flow vorticity by the lateral pressure gradient and boundary layer cross flow effects

(Fig. 6); (b) assessment of the validity of the independence principle and the influence of deviations from it due to compressibility and cross-flow turbulence effects as a function of sweep angle, yielding predictions in good agreement with experiment (Fig. 7); (c) examination of the 3-D skin friction line behavior and approach to separation (Fig. 8), including a satisfactory prediction of the enhanced incipient separation due to shock sweep (Fig. 9); and (d) a new universal solution for the inner viscous/turbulent shear disturbance deck that accounts exactly for the cross-flow to streamwise eddy viscosity ratio effect over the entire range of sweep angles. The similtude properties of these swept interactions as regards Mach Number and Reynolds Number Effects were also investigated, reported on at a 1986 AIAA Meeting and documented in AIAA Paper 86-0395 (Ref. 11).

Our investigation was next broadened to consider the case of conically-symmetric shock interactions (Fig. 10). Since it is an important experimental question and of basic theoretical significance as well, we particularly addressed the problem of the so-called "inception distance" in such interactions (see Figure 11). A fundamental analysis of the governing viscous-inviscid interaction equations in an appropriate shock-oriented spherical coordinate system revealed a number of important physical features concerning the radial and far-field behavior of such interactions. Moreover, this analysis served to derive an experimentally verified prediction of the inception-length dependence on the upstream influence scale normal to the shock and the sweep angle. A paper on this work was presented at the 1986 USAF/FRG D.E.A. meeting at Dayton, Ohio and the 10th U.S. National Applied Mechanics Congress at the University of Texas (both in June 1986) and subsequently published in early 1987 by the AIAA Journal.[12]

The aforementioned study of the outboard radial-inception length problem for swept shocks has been accompanied by an analytical study focused on the inboard, highly-nonconical (or noncylindrically-symmetric) interactive region near the shock generator in order to gain a basic understanding of its interactive physics and the resulting inception distance phenomena: as shown clearly by our far field analysis, only detailed study of this region can reveal the specific quantative dependence of ℓ_{incept} on Mach Number, Reynolds Number, and shape of the incoming boundary layer profile. To fix ideas, this study addressed the specific problem of the corner region formed by a thin fin on a wall (Figure 12) for a supersonic, adiabatic laminar unseparated interaction. The study was being carried out as the Ph.D. dissertation work of Mr. S. Ahmed using a 3-D triple-deck and double Fourier-transform method of approach. At the time of contractual termination, the entire spectrum of the solution in the Fourier Plane had been completed and was undergoing inversion to obtain the streamwise and lateral physics including the upstream influence characteristics and skin friction lines.

Further understanding of the underlying physical trends governing swept shock-boundary layer interactions was obtained by working out a direct comparison of our turbulent triple deck theory with the $M_\infty = 2.85$ small compression corner interaction 2-D flow data of Settles.[13] As shown in Figure 13, the theory is in excellent agreement with experiment over a wide range of large Reynolds Numbers. Also in evidence in this Figure is the fact that such comparisons are sensitive to the shape of the incoming turbulent boundary layer profile. Accordingly, we have also made a detailed study of <u>this</u> question by recasting our entire theory in terms of Law of the Wall/Law of the Wake Parameters and then examining the influence of the Outer Wake Function and Inner Deck Turbulence Modeling, respectively, on the predicted interaction

properties. Typical results taken from the documenting AIAA Paper (attached as Appendix C), are illustrated here in Figures 14 and 15 for the upstream influence distance of 2-D interactions; these results clearly indicate that the wake function in particular must be accurately known to affect meaningful experimental/theoretical comparisons in high Reynolds Number flows. This work has had a significant impact on the planning of future experimental and CFD studies of shock/boundary layer interactions (see Appendix D).

The aforementioned Law of the Wall/Wake similtude version of our turbulent triple deck theory was subsequently extended to 3-D swept interactions with either cylindrical or conical symmetry. Typical results from this work, which was documented in Ref. 14, are given in Figures 16 and 17 to illustrate the influence of Mach number and shape factor, respectively, over the sweepback effect on interactive upstream influence distance.

2.3 Complementary Activities

As an outgrowth of an earlier AFOSR-sponsored two-month visit in 1984 by Dr. Nandanan (a previous collaborator), in which we devised a new theoretical approach for predicting interaction-zone slot suction effects on supercritical airfoils, a joint paper was prepared on our work and subsequently presented to the May 1986 AIAA/ASME Fluid Mechanics and Plasma Dynamics Meeting in Atlanta (Figure 18). Dr. Nandanan was also invited to present the work at the Summer of 1986 Asian Fluid Mechanics Meeting in Tokyo. This exploratory research could prove a significant guide to future studies of the use of localized suction control of 3-D interactions.

Another auxiliary investigation completed under the partial auspices of this contract was an extension of the triple deck theory to treat moderately hypersonic shock/laminar boundary layer interactions. The results, which

were presented to an AIAA meeting and documented in Paper 88-0603 (Figure 19), will serve to guide subsequent studies of hypersonic turbulent 3-D interactions.

Finally, it is important to mention a significant and unique aspect of this research throughout its execution: the AFOSR-encouraged cooperation with selected other investigators working in parallel on the problem, namely Professors G. Settles, D. Dolling and S. Bogdonoff (experimental studies) and Dr. C. M. Horstman and Prof. D. Knight (CFD studies). This further resulted in a newly-formed AIAA Ad-hoc High Speed Flow Panel that meets twice a year at the Summer and Winter AIAA Meetings, and also in two successive two-day summer 3-D Shock/Turbulent Boundary Layer Interaction Workshops at Penn State (1987) and Princeton University (1988).

3. SUMMARY AND CONCLUSION

The triple-deck approach embodied in this interaction study part of this project has enabled the successful analysis of non-separating 3-D SBLI's including the basic features of:

- Turbulence modeling in the middle deck (wake function effect);
- Turbulence modeling in the inner deck (Law of the Wall aspects, including non-isotropy effects and the influence of the cross-flow turbulence);
- Streamwise vorticity generation and skin friction line geometry prediction;
- Determination of the similtude laws for ℓ_u/δ_o & $Cp_{i,s} = F_{NS}(\Lambda, Re_\delta, M_{e_1}$ and $\pi_1)$ over a wide range of conditions.

In particular, our results have yielded fundamental understanding of sweep effects, showing that: (a) upstream influence increases rapidly with sweepback, a major contributor to this being the cross-flow interactive turbulence effect; (b) significant deviations from independence principle-predictions can occur for $\Lambda > 30^o$, due to a combination of compressibility effects on variable fluid properties and the interactive cross-flow turbulence effect; (c) a pronounced decrease in incipient separation pressure (i.e. "earlier" separation) with sweep is predicted in good agreement with experiment.

REFERENCES

1. Inger, G. R., "Three-Dimensional Disturbances in Reattaching Separated Flow," Proc. AGARD Symposium on Flow Separation, CP-168, pp. 18-1 to 18-12.

2. Inger, G.R., "Three-Dimensional Heat and Mass Transfer Effects Across High Speed Reattaching Flows," VPI&SU Report Aero-036, Blacksburg, Va., July 1975. Presented as AIAA Paper 76-160, 14th Aerospace Sciences Meeting, Washington, D.C., January 1976; AIAA Journal 15, March 1977, pp. 383-389.

3. Namtu, M. and G. R. Inger, "Spanwise-Periodic Three-Dimensional Disturbances in Nominally 2-D Separating Laminar Boundary Layer Flows," VPI&SU Report Aero-052, Blacksburg, Va., August 1976.

4. Inger, G. R., "On the Curvature of Compressible Boundary Layer Flows Near Separation," Zeitschrift für Agenwante Mekanik and Physik ("ZAMP"), Vol. 286, 1977, pp. 1027-1035.

5. Inger, G. R., "Compressible Laminar and Turbulent Boundary Layers Near Separation or Reattachment," AIAA Paper 78-1164, 11th Fluid and Plasma Dynamics Conference, Seattle, July 1978.

6. Inger, G. R., "A Theoretical Study of Spanwise-Periodic 3-D Disturbances in the Wake of a Slightly-Stalled Wing," Proc. International Conf. on Aerodynamics at Low Reynolds Numbers, Royal Aeronautical Society, London, Oct. 1986.

7. Fannelop, T.K., "Effects of Streamwise Vortices on Laminar Boundary Layer Flow," Trans. ASME Jour. App. Mech., June 1968, pp. 424-426.

8. Inger, G. R., "Analytical Investigation of Swept Shock-Turbulent Boundary Layer Interaction in Supersonic Flow," AIAA Paper 84-1555, 1984.

9. Inger, G. R., "Supersonic Viscous-Inviscid Interaction of a Swept Ramp with a Turbulent Boundary Layer," AIAA Paper 85-1669, 1985.

10. Inger, G. R., "Supersonic Viscous-Inviscid Interaction of a Swept Compression Ramp with a Turbulent Boundary Layer," Turbulent Shear Layer/Shock Wave Interactions, IUTAM Symposium, Palaiseau 1985, (Ed. J. Délery), Springer, Berlin Heidelberg 1986.

11. Inger, G. R., "Incipient Separation and Similtude Properties of Swept Shock/Turbulent Boundary Layer Interactions, AIAA Paper 86-0345, Reno, Jan. 1986.

12. Inger, G. R., "Incipient Separation and Similtude Properties of Swept Shock/Turbulent Boundary Layer Interactions," AIAA Paper 86-0345, 1986.

13. Inger. G. R., "Spanwise Propagation of Upstream Influence in Conical Swept Shock/Boundary Layer Interactions, "AIAA Journal 25, Feb. 1987, pp. 287-293.

14. Inger, G. R., "The Role of Law of the Wall/Wake Modeling in Validating Shock-Boundary Layer Interaction Predictions," AIAA Paper 88-3581, July 1988.

15. Smits, A. (ed.), "Meeting at the Working Group on 3-D Shock Wave/Turbulent Boundary Layer Interactions," Princeton University, Dept. of Mechanical and Aerospace Eng. Report, July 1988.

The Royal Aeronautical Society
4. Hamilton Place. London. W1V 0BQ Tel. 01-499 3515

INTERNATIONAL CONFERENCE AERODYNAMICS AT LOW REYNOLDS NUMBERS
($10^4 < Re < 10^6$) - 15th - 17th OCTOBER 1986

A theoretical study of spanwise — periodic 3-D disturbances in the wake of a slightly stalled wing at low Reynolds numbers
G. R. Inger

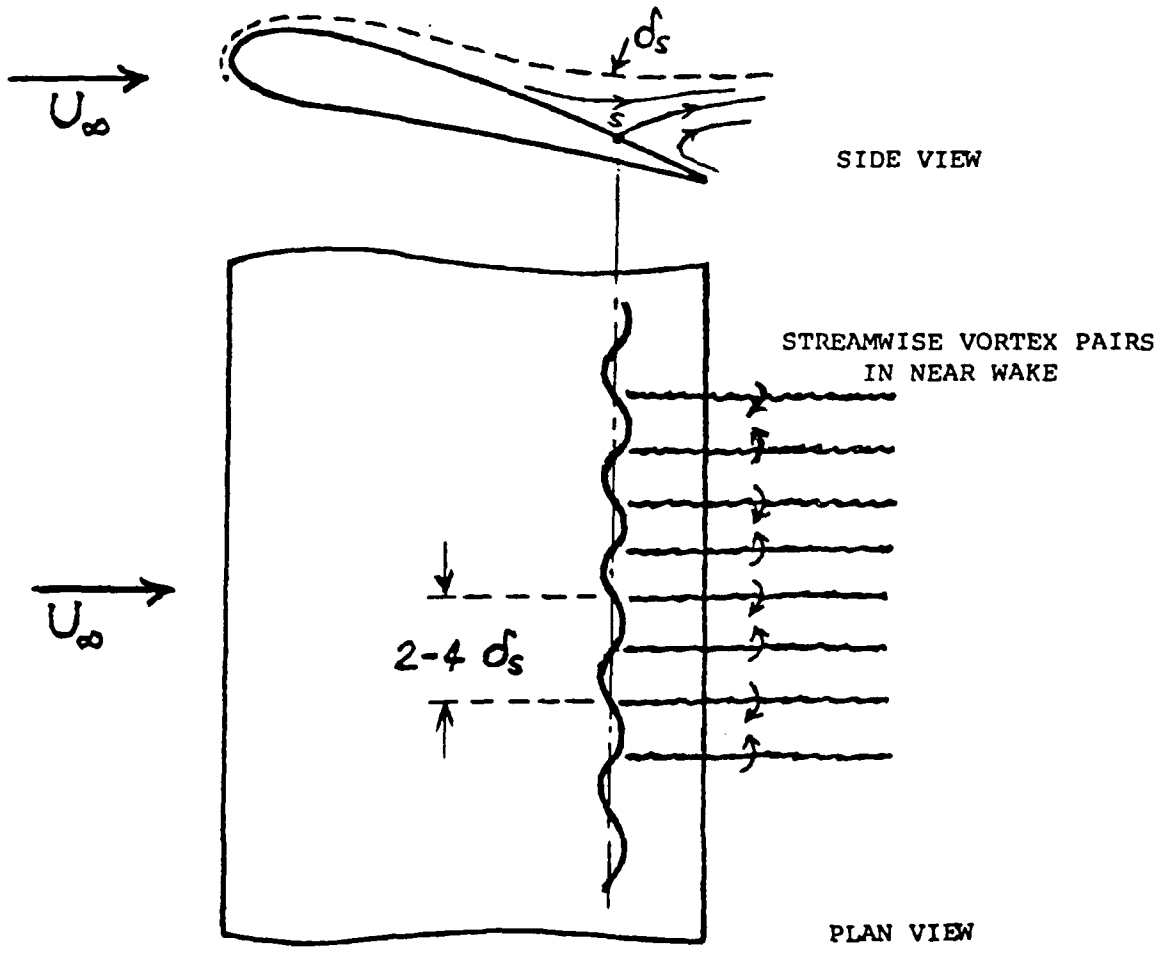

Fig. 1

A theoretical study of spanwise-periodic disturbances in Falkner-Skan boundary-layer flows

Masafumi Konno

A Thesis Submitted to the
Graduate Faculty in Partial Fulfillment of the
Requirements for the Degree of
MASTER OF SCIENCE

Iowa State University
Ames, Iowa

1987

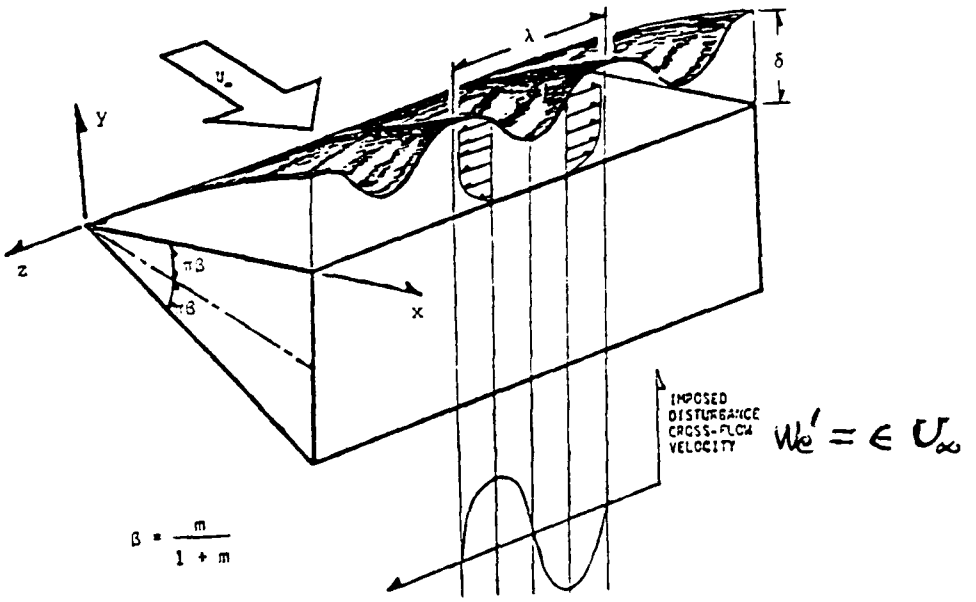

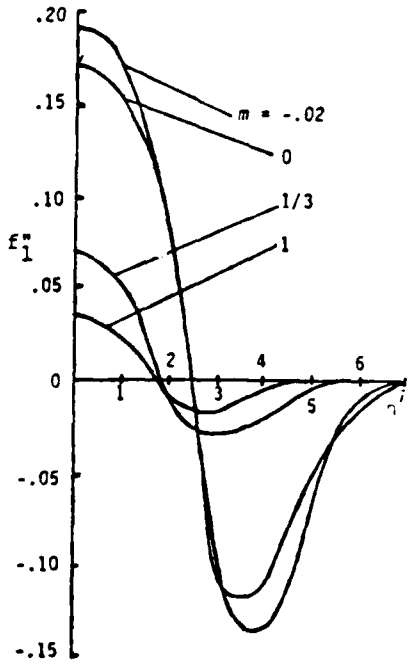

$$C_{f_x} = 2\frac{1}{\sqrt{Re_x}}\{f_0''(0) + \epsilon\left[\sum_{i=1}^{\infty} a^{1-i}\xi^i F_i''(0)\right]\cos\left(\frac{2\pi z}{\lambda}\right)$$

Fig. 2

AIAA'87

AIAA-87-0285

Non-Isotropic Effects in the Wall Region of a Three-Dimensional Turbulent Boundary Layer

G.R.Inger and S.Ahmed

Iowa State University, Ames, IA

$$u^* \simeq B_u + \frac{1}{ka}\ln y^* + \frac{\alpha_x y^*}{2k}\left\{1 + \frac{R_\tau(R_\tau - R_p)}{a^2}\left[1 + 2\varepsilon\frac{G(y^*)}{y^*}\right]\right\}$$

$$w^* \simeq B_w R_\tau + \frac{R_\tau}{ka}\ln y^* + \frac{\alpha_x y^*}{2k}\left\{R_p - \frac{(R_\tau - R_p)}{a^2}\left[1 + 2\varepsilon\frac{G(y^*)}{y^*}\right]\right\}$$

$$\epsilon \equiv 1 - T$$

where $G(y^*)$ is the positive quantity

$$G(y^*) = \int_0^{y^*}\left(\frac{\ln y^* + Bu_o k - 1 - \frac{2\lambda k}{y^*}}{Bu_o + \frac{1}{k}\ln y^*}\right) dy^*$$

and

$$B_u = B_{uo}\left[\frac{1}{a} + C_1\frac{\alpha_x}{2K}\left\{1 + \frac{R_\tau(R_\tau - R_p)}{a^2}\left\langle\left(1 + 2C_2(1-T)\right\rangle\right\}\right]$$

$$B_w = B_{uo}\left[\frac{R_\tau}{a} + C_1\frac{\alpha_x}{2K}\left\{R_p - \left(\frac{R_\tau - R_p}{a^2}\right)\left\langle 1 + 2C_3(1-T)\right\rangle\right\}\right]$$

where $Bu_o = 5.2$ for $k = .41$ and $C_1/2K = 2.68$

$C_2 = 2.39$, $C_3 = 3.58$

Fig. 3

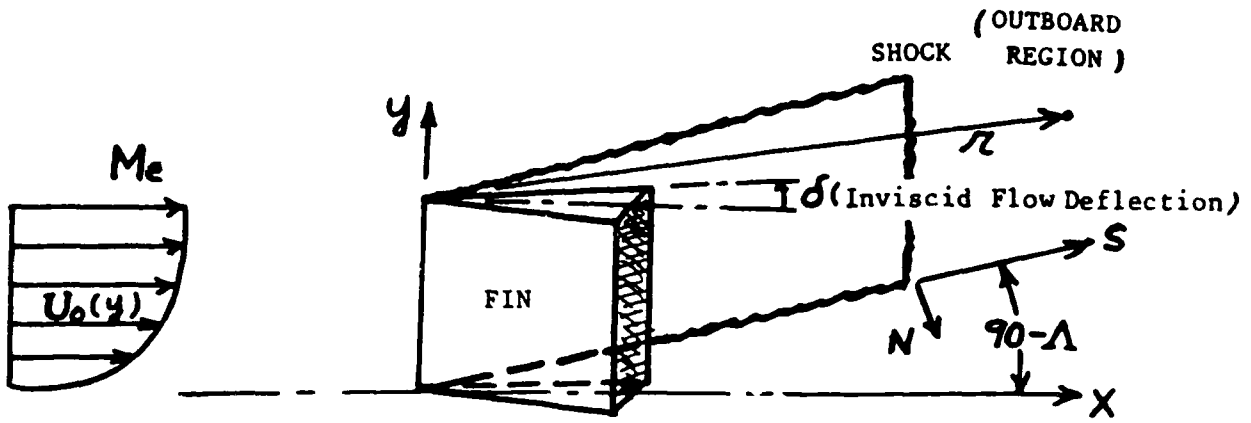

A. Fin-Generated Shock

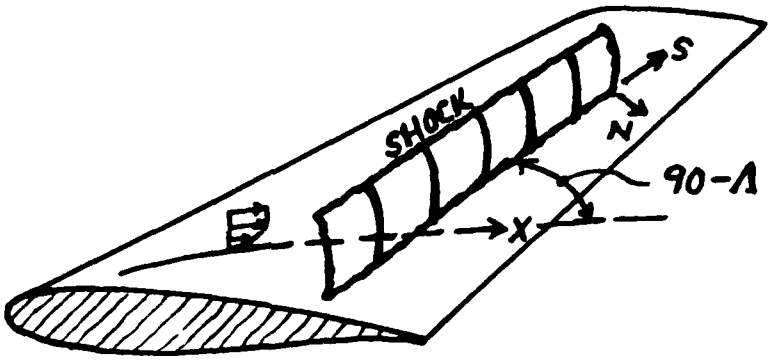

B. Supercritical Swept Wing

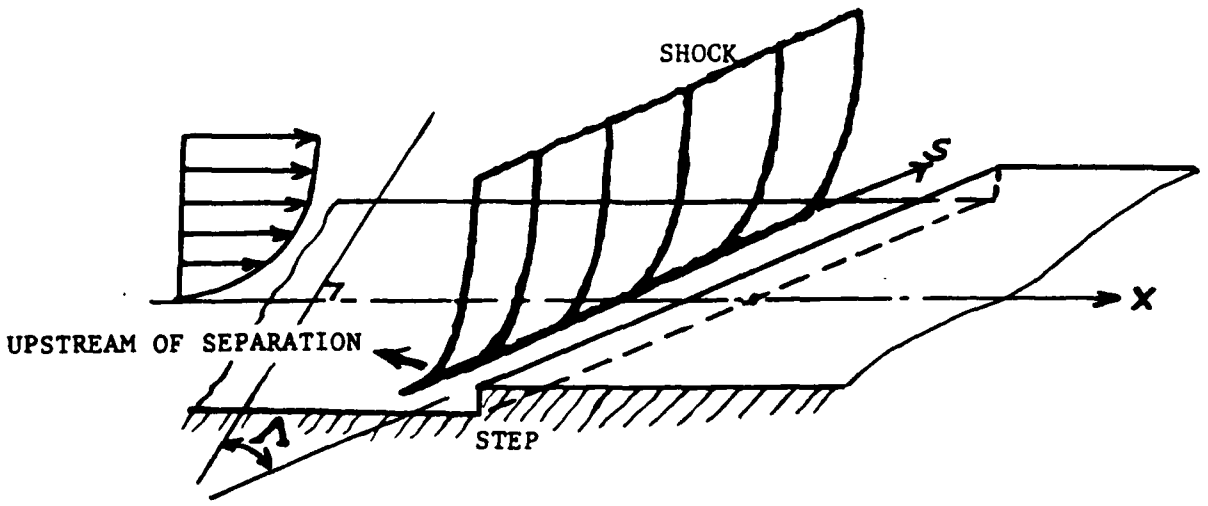

C. Small Foreward-Facing Step

Fig. 4 Example Applications of the Swept Shock/Turbulent Boundary Layer Theory

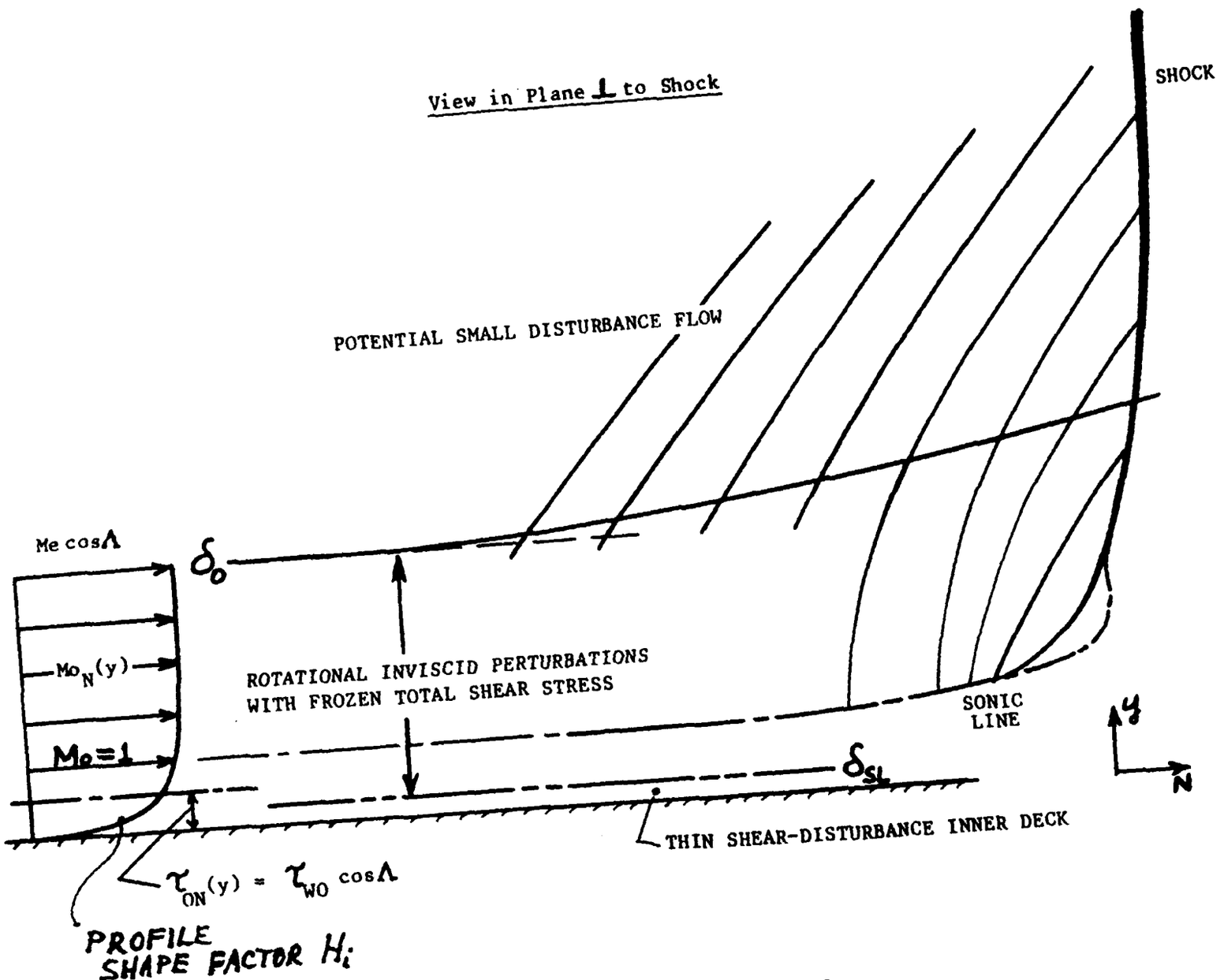

Fig. 5 Triple-Deck Structure of the Interaction

STREAMWISE VORTICITY

$$\Omega_x' \equiv \frac{\partial w'}{\partial y} - \frac{\partial v'}{\partial z}$$

$$\frac{\partial \Omega_x'}{\partial x} \simeq -\frac{d(\rho_0 U_0)/dy}{\rho_0 U_0(y)} \cdot \frac{\partial w'}{\partial x}$$

$$\Omega_x'(N,y) \simeq -\sin\Lambda \frac{d(\rho_0 U_{0N})}{dy} \frac{p'(N)}{(\rho_0 U_{N_0})^2}$$

CROSS FLOW DISTURBANCE OF A NON-UNIFORM INCOMING STREAM GENERATES STREAMWISE VORTICITY

VERY SENSITIVE TO INCOMING PROFILE

CROSS-FLOW ANGLE

$$\beta \simeq \sin\Lambda \left[\frac{p_w'(x)}{\gamma p_1}\right] \cdot U_{N_0}(y)/M_{N_0}^2(y)$$

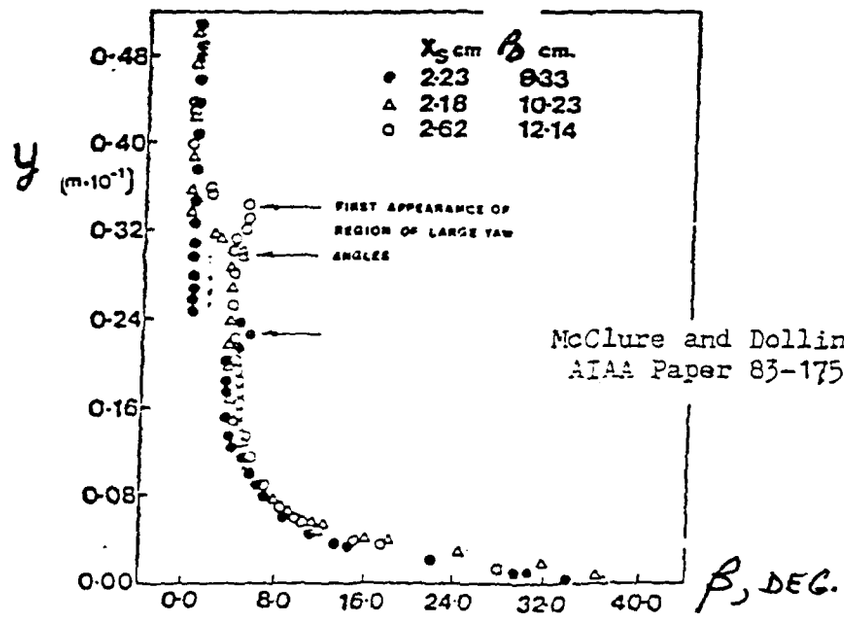

McClure and Dolling
AIAA Paper 83-1754

Fig. 6

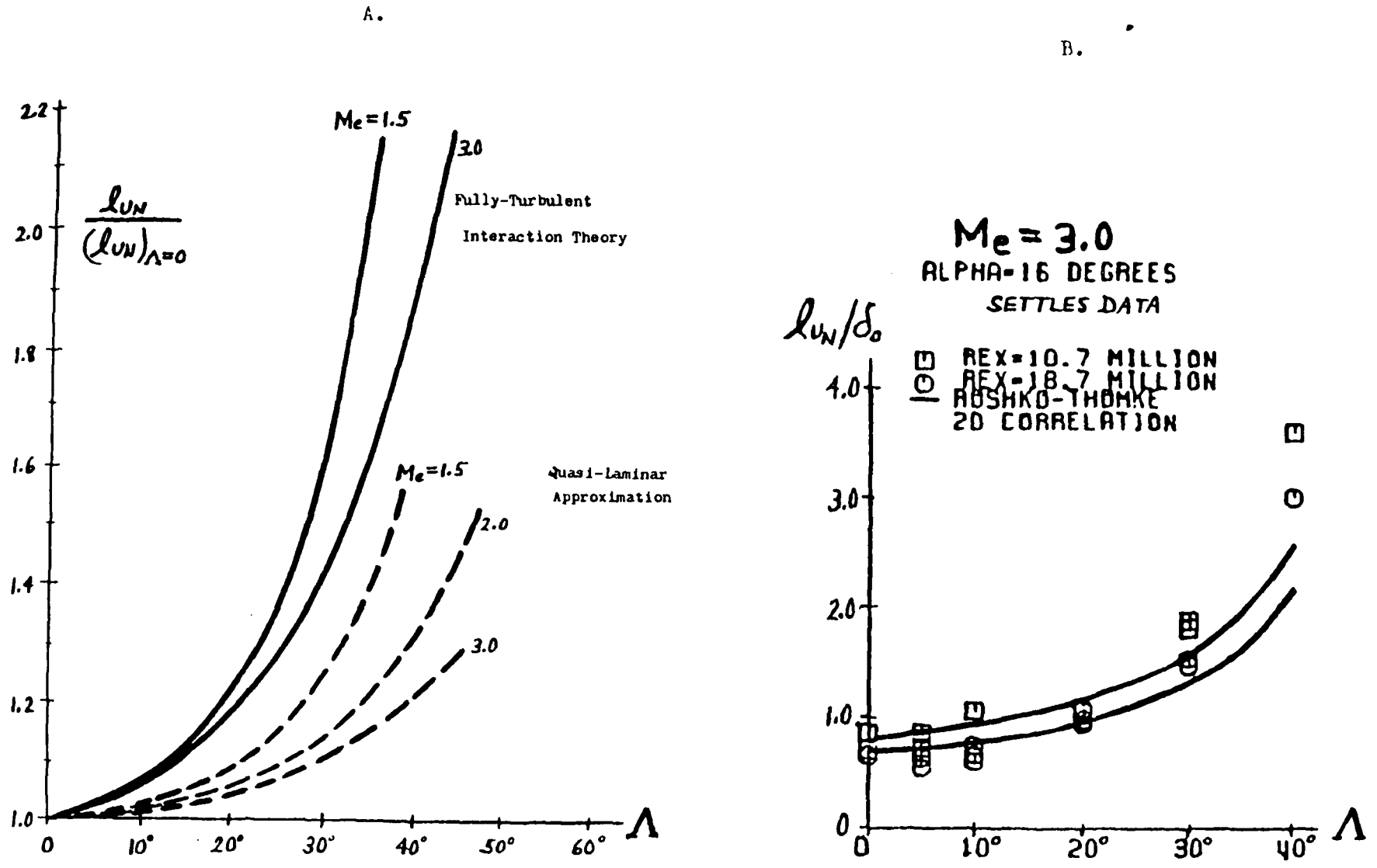

Fig. 7

Predicted and Experimental Results for the Sweepback Effect on Upstream Influence

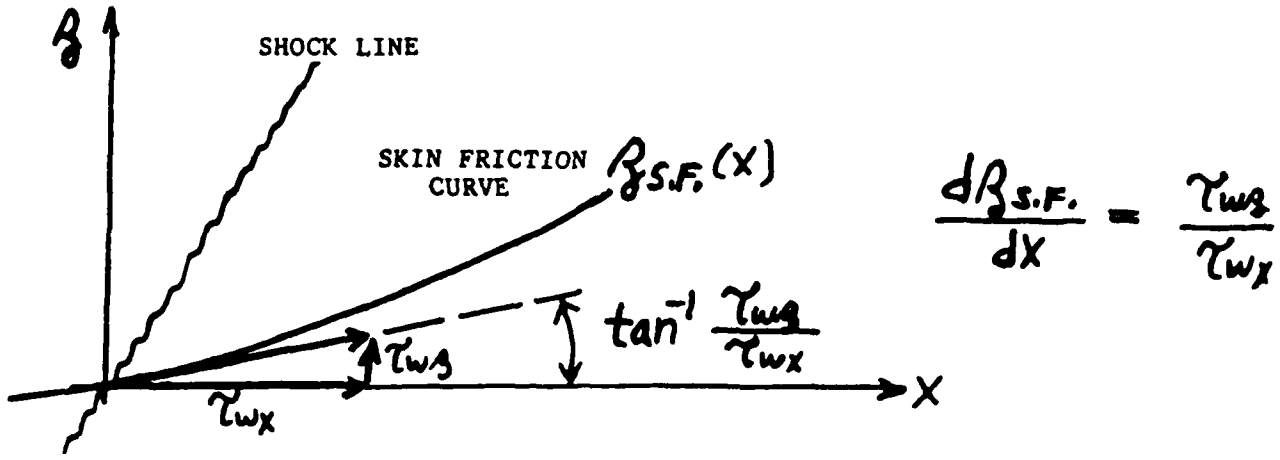

Definition of Skin Friction Line Geometry

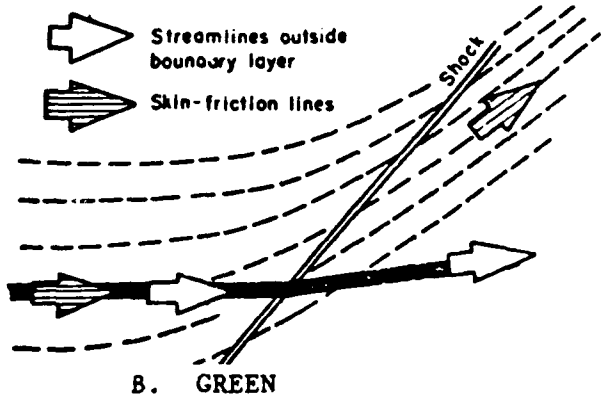

B. GREEN

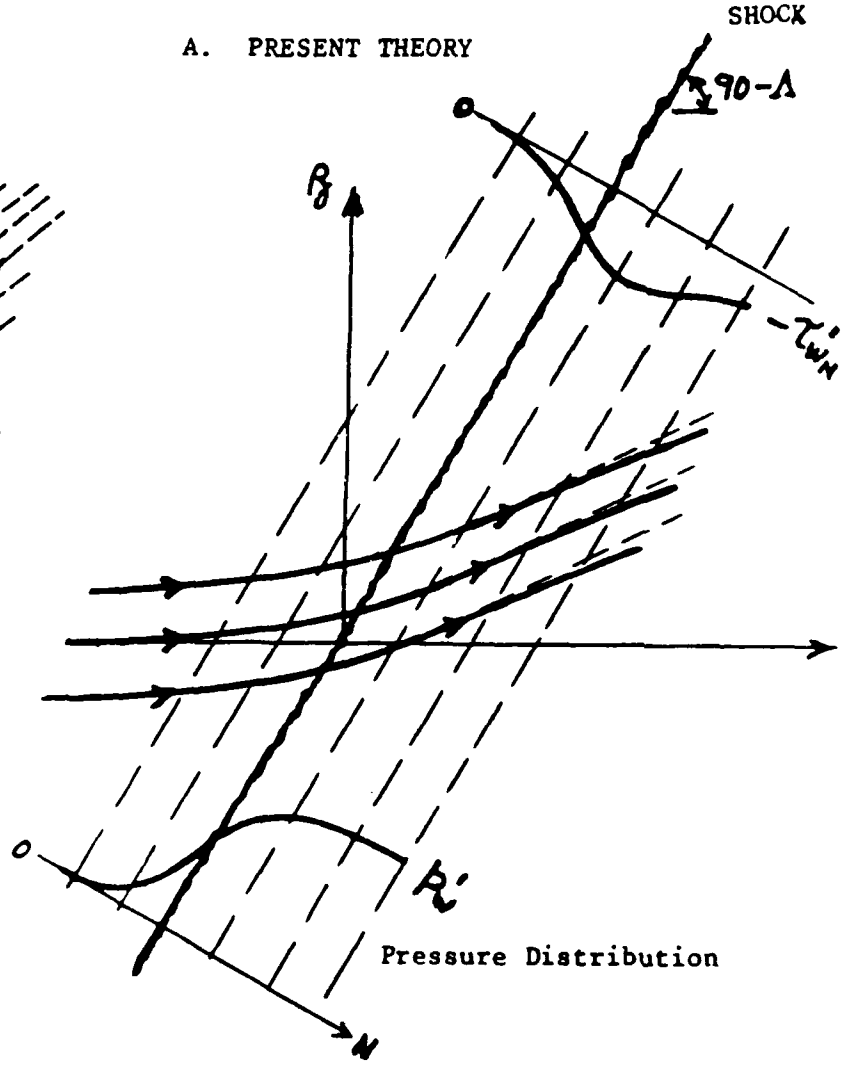

Typical Non-Separating Interaction Skin Friction Line Behavior

Fig. 8

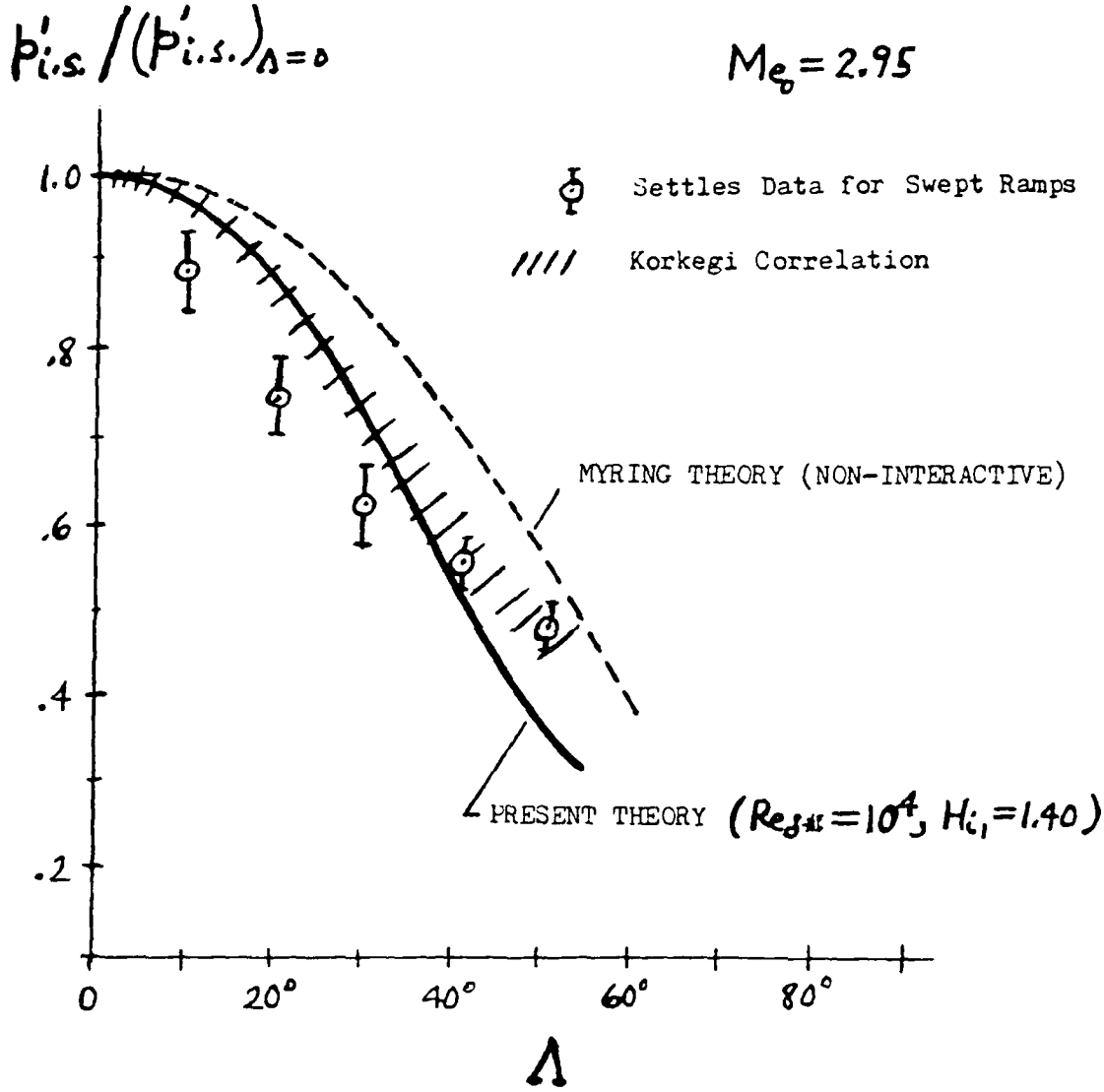

Fig. 9

Incipient Separation Pressure variation with Sweepback Angle

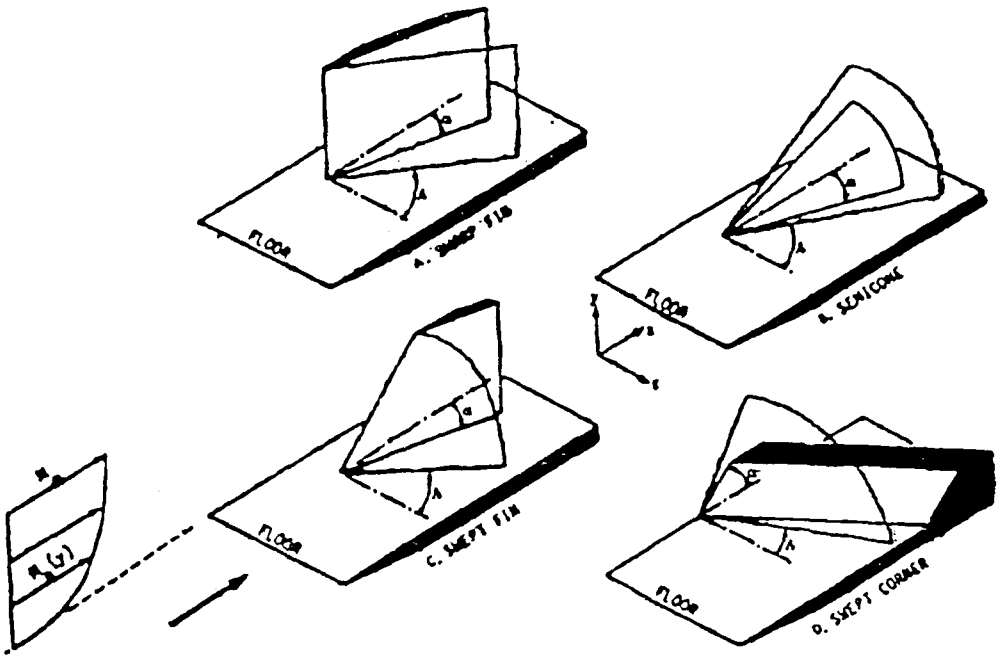

Fig. 10

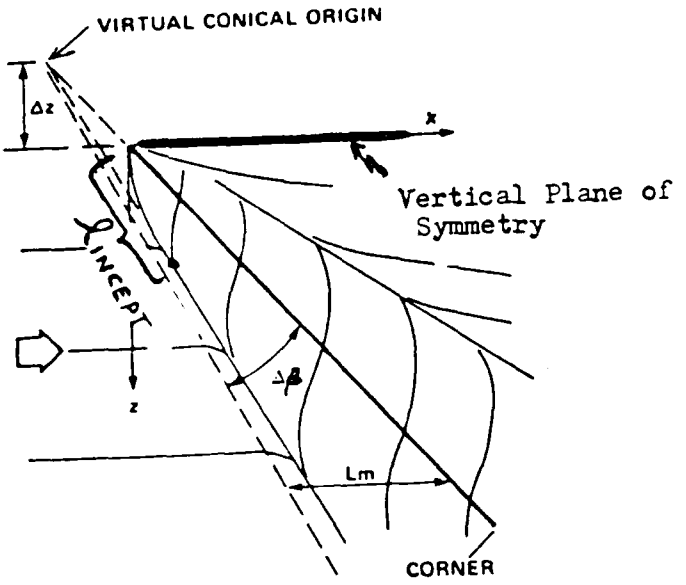
VIRTUAL CONICAL ORIGIN
Δz
x
Vertical Plane of
Symmetry
INCEPT
z
Δβ
Lm
CORNER

Fig. 11

FUNDAMENTAL THEORY OF FIN-INDUCED SHOCK WAVE - BOUNDARY LAYER INTERACTION

THE PROBLEM

- VERY TALL SHARP SLENDER FIN (δ SMALL)
- HIGH REYNOLDS NUMBER LAMINAR FLOW
- NON-SEPARATING FLOW
- STEADY ADIABATIC SUPERSONIC FLOW

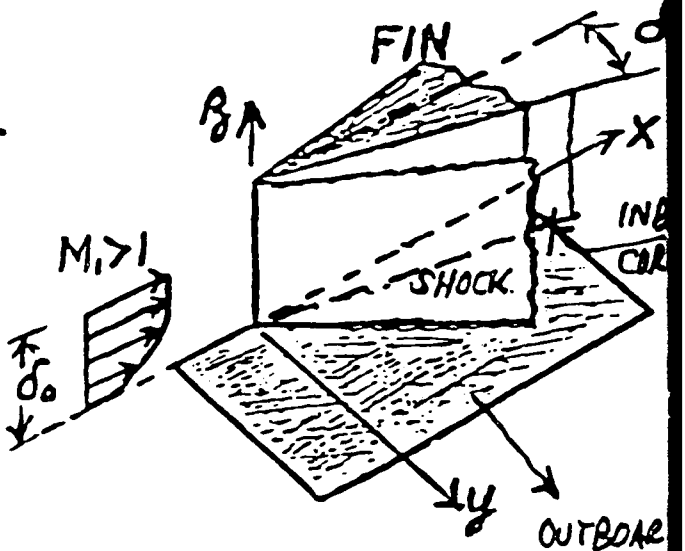

CONTENTS

- BASIC TRIPLE-DECK STRUCTURE OF THE INTERACTION FIELD
- SET-UP OF THE BOUNDARY VALUE PROBLEM CHARACTERIZING THE FIN PROBLEM
- SOLUTION TECHNIQUE BY FOURIER-TRANSFORM METHODS

OBJECTIVES

- UNDERSTAND THE 3-D EFFECTS
- PROVIDE A PHYSICALLY-ORIENTED ANALYTICAL FRAMEWORK
- ULTIMATELY TO PREDICT INTERACTIVE THICKENING EFFEC WALLSKIN FRICTION LINES & 3-D INCIPIENT SEPARATIO

Fig. 12

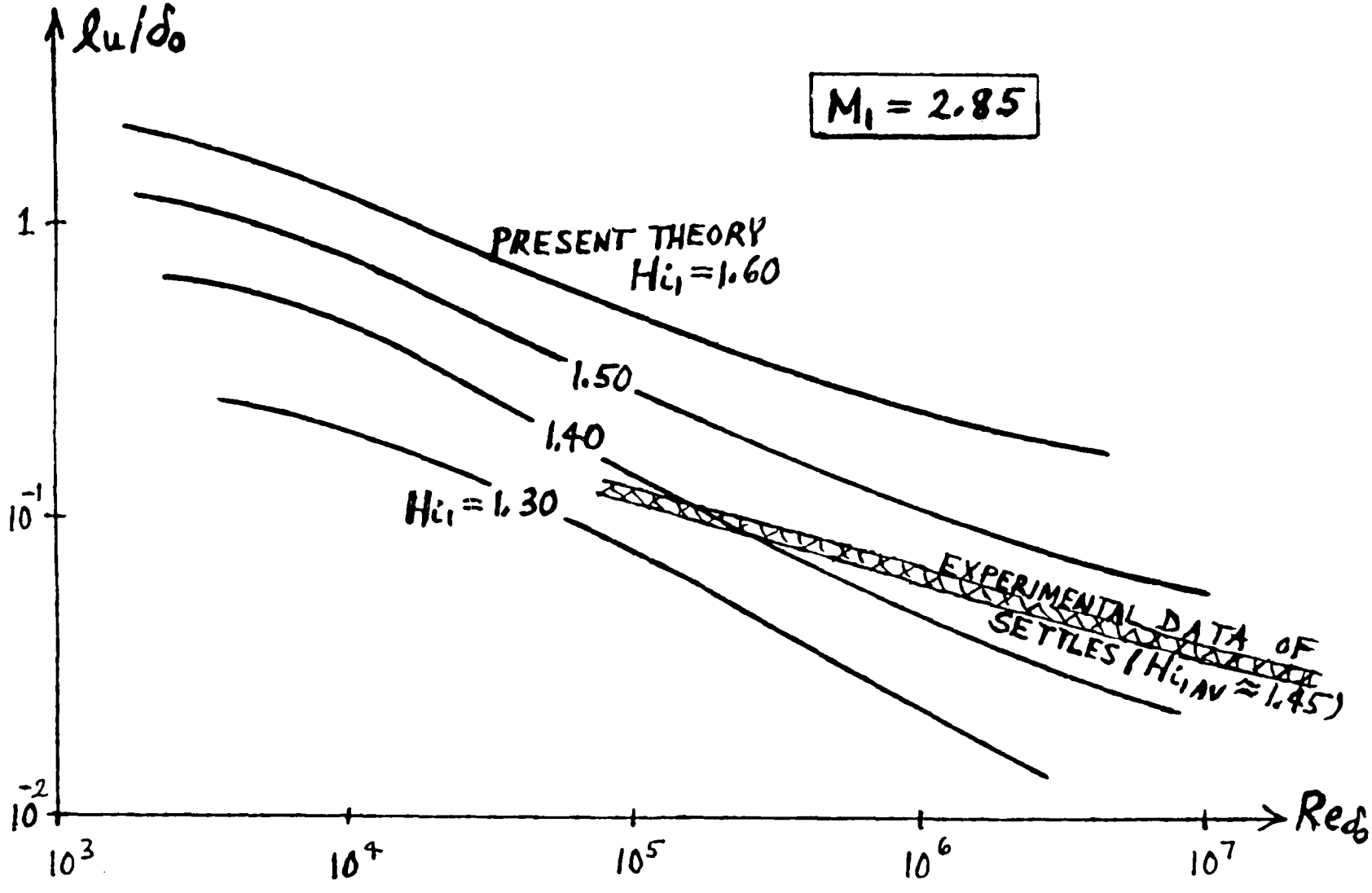

Fig. 13

TYPICAL SHAPE FACTOR EFFECT ON THE EXPERIMENTAL VALIDATION OF PREDICTED UPSTREAM INFLUENCE VS. REYNOLDS NUMBER (WEAK COMPRESSION CORNERS).

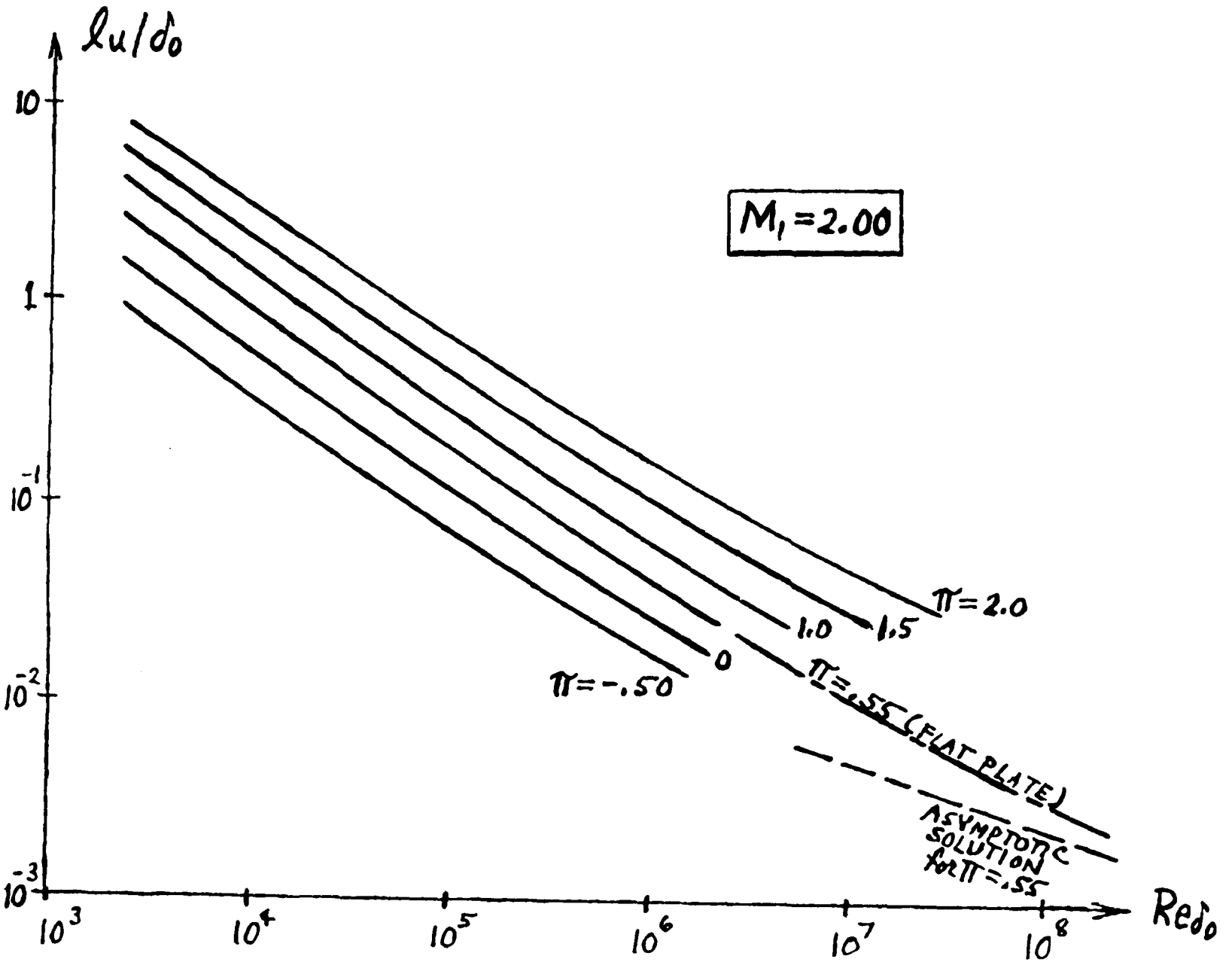

Fig. 14

PREDICTED WAKE FACTOR EFFECT ON THE UPSTREAM INFLUENCE OF NON-SEPARATING SHOCK-TURBULENT LAYER INTERACTIONS AT MACH TWO

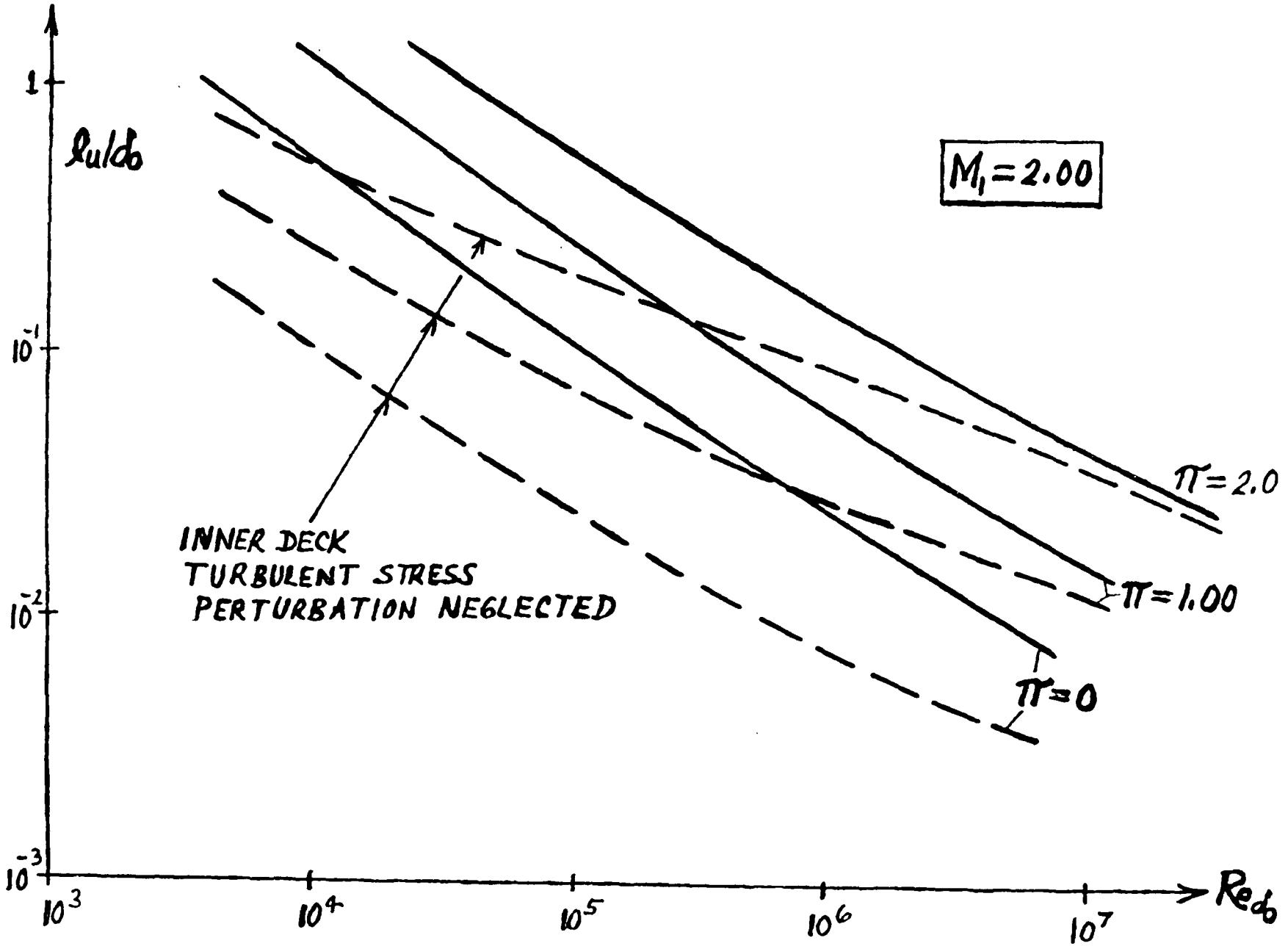

Fig. 15

TYPICAL EFFECT OF THE TURBULENT EDDY VISCOSITY DISTURBANCE

IN THE INNER LAW OF THE WAKE REGION ON VELOCITY PROFILES

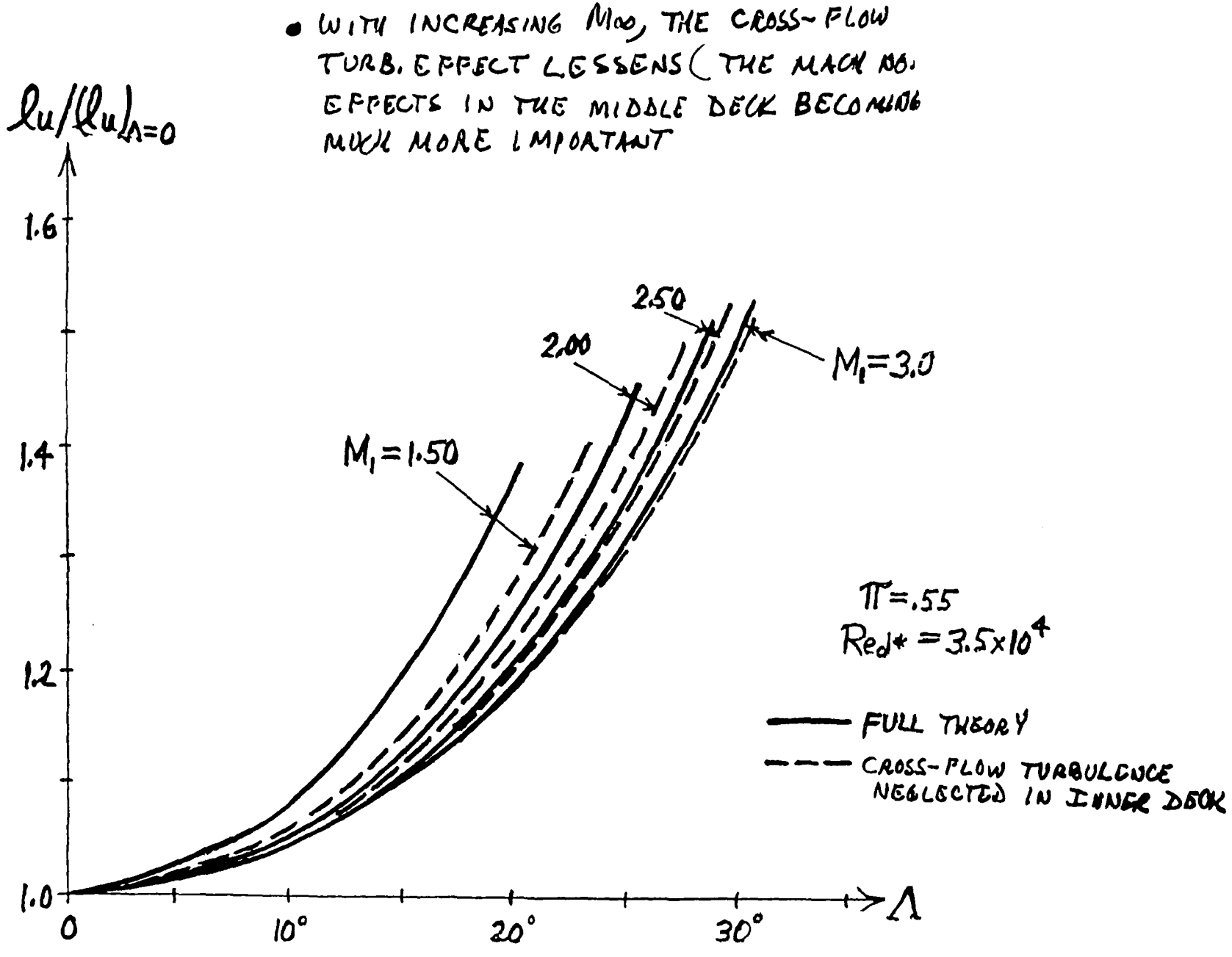
• WITH INCREASING M_∞, THE CROSS-FLOW TURB. EFFECT LESSENS (THE MACH NO. EFFECTS IN THE MIDDLE DECK BECOMING MUCH MORE IMPORTANT
$l_u/(l_u)_{\Lambda=0}$
1.6
1.4
1.2
1.0
0
10°
20°
30°
Λ
2.50
2.00
$M_1=3.0$
$M_1=1.50$
$\pi=.55$
$Re_{\delta^*}=3.5\times10^4$
FULL THEORY
CROSS-FLOW TURBULENCE NEGLECTED IN INNER DECK

Fig. 16

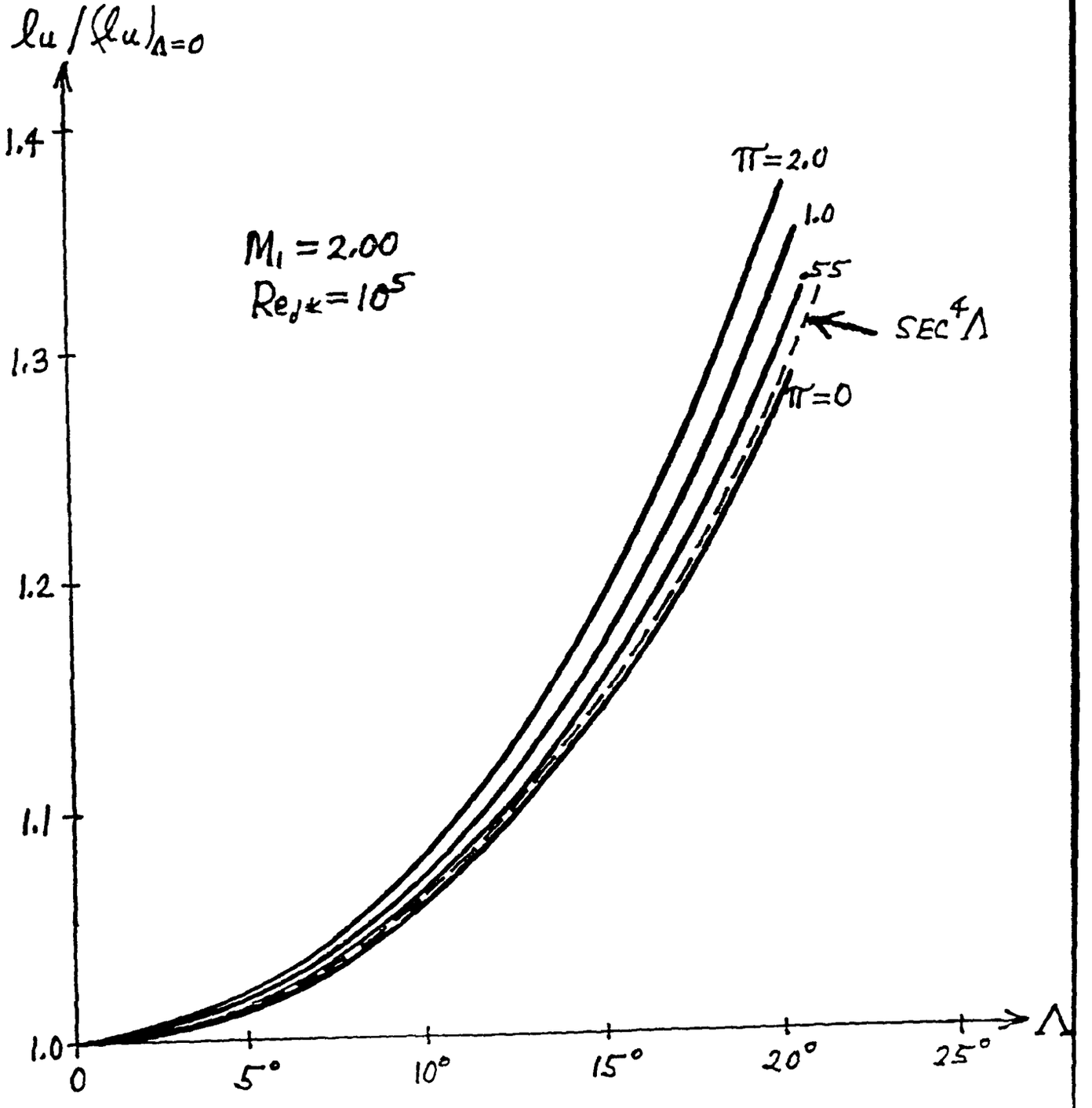
$\ell u / (\ell u)_{\Lambda=0}$
1.4
1.3
1.2
1.1
1.0
$M_1 = 2.00$
$Re_{/\ell} = 10^5$
$\pi = 2.0$
1.0
.55
$SEC^4 \Lambda$
$\pi = 0$
0
5°
10°
15°
20°
25°
Λ

Fig. 17

AIAA-86-1035

Prediction of Local Suction Effects on Transonic Shock/Turbulent Boundary Layer Interaction and Downstream Flow

G.R. Inger and M. Nandanan,
Iowa State Univ., Ames, IA

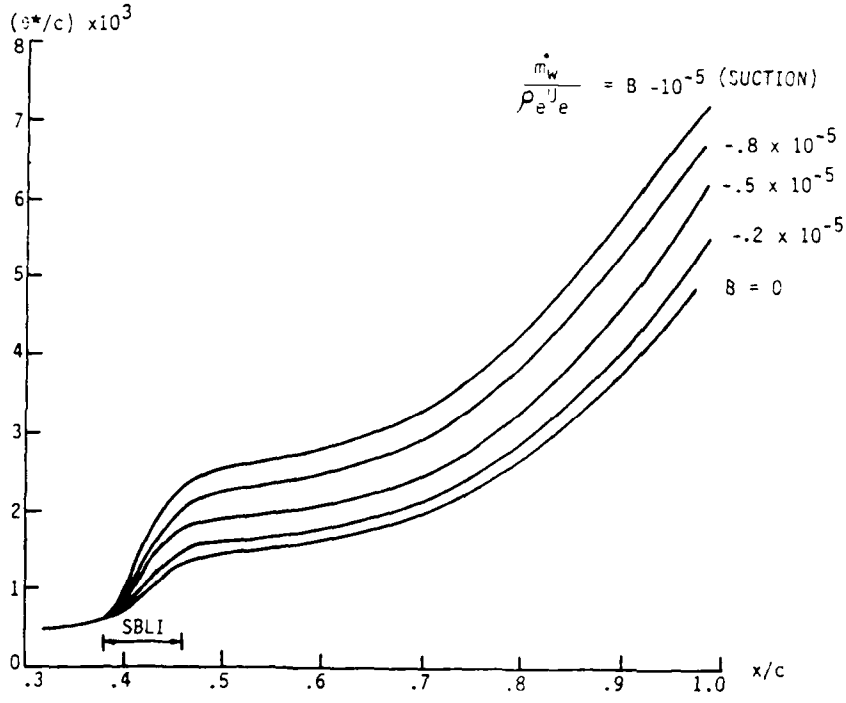

Influence of SBLI Zone [illegible] on Downstream Momentum Thickness

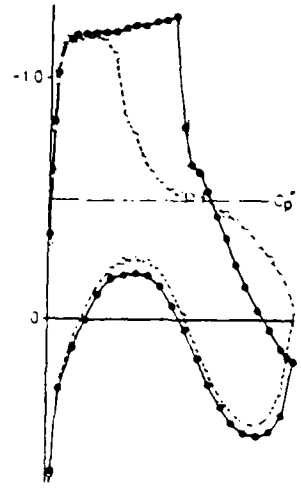

AIRFOIL VFW VA-2 WITH DOUBLE SLOT

$M_\infty = 0.78$ $Re_\infty = 2.5 \cdot 10^6$

FIXED TRANSITION
3/.25c , 180K

DATA
- - - WITHOUT CONTROL
——●—— WITH SUCTION
$c_Q = 0.0006$

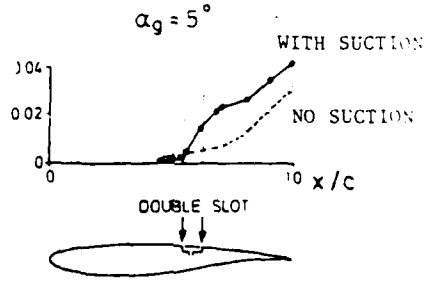

Fig. 18

AIAA'88

AIAA-88-0603

Oblique Shock/Laminar Boundary Layer Interactions in Hypersonic Flow

G.R. Inger and A.A. Rangwalla
Iowa State University, Ames, IA

AIAA 26th Aerospace Sciences Meeting
January 11-14, 1988/Reno, Nevada

Fig. 19

APPENDICES

APPENDIX A

ABSTRACT

"THEORY OF STEADY SPANWISE-PERIODIC
DISTURBANCES IN FALKNER-SKAN BOUNDARY LAYERS"

G. R. Inger and M. Konno*
Iowa State University
Ames, Iowa 50011
United States of America

This work describes a theoretical investigation of the effect of weak spanwise-periodic cross flow disturbances in the freestream above a high Reynolds number laminar boundary layer on a wedge-shaped body. Our emphasis is on a careful treatment of the spanwise-gradient viscous effects in the perturbation field for arbitrary values of the spanwise wavelength. In addition to explaining and eliminating a heretofore-puzzling singularity encountered in previous studies of this flow problem, we also bring out how the host flow pressure gradient influences the 3-D disturbance effect on such properties as the skin friction and displacement thickness distributions.

*Glenn Murphy Distinguished Professor and Graduate Research Assistant, respectively, Dept. of Aerospace Engineering.

EXTENDED SUMMARY

"THEORY OF STEADY SPANWISE-PERIODIC

DISTURBANCES IN FALKNER-SKAN BOUNDARY LAYERS"

1. Introduction

Thorough understanding of 3-D disturbance effects on a laminar boundary-layer is an important problem in fluid mechanics. In particular, it is of interest in the aerodynamic design of both aircraft and turbomachinery to formulate an analytical model of streamwise vorticity effects on the properties of an underlying boundary layer.

Crow [1] investigated a weak periodic transverse flow effect on a flat-plate boundary layer using a perturbation expansion of the full Navier-Stokes equations for steady, incompressible, viscous flow. Fannelop [2] then simplified the governing equations for this problem by a boundary-layer type approximation (i.e., $\partial p/\partial y = 0$ and $\mu \partial^2 u/\partial x^2 \simeq 0$) and obtained an equivalent result as Crow. In both works, the spanwise viscous derivatives and the perturbation pressure were neglected, and the resulting predictions of three-dimensional effects were shown to grow unbounded downstream, suggesting a breakdown of their analysis.

The present work analyzes the effects of a weak steady periodic transverse flow on the incompressible laminar Falkner-Skan boundary layer along a wedge [Fig. 1]. We formulate the problem by also adopting a high Reynolds number boundary layer approach and introducing a small perturbation expansion in the simplified governing equations. However, in our approach we retain

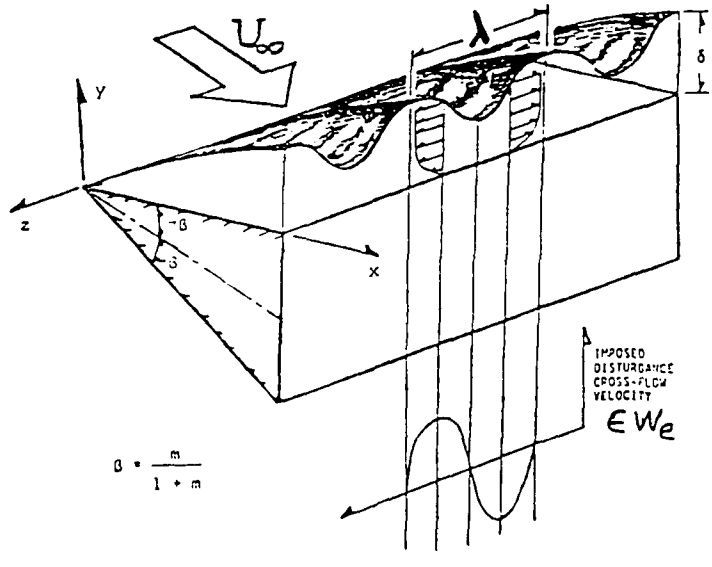

Figure 1: Sketch of the flow model and coordinate system.

and carefully treat the pressure perturbation and the viscous z-derivative effects for arbitrary spanwise wave lengths, since the downstream disturbance development strongly depends on these effects as shown later.

We first re-investigate the limiting case of flatplate flow to explain and eliminate the solution singularity. Correct numerical solutions are obtained using an iterative outward shooting method developed by Nachtsheim and Swigert [3]. Qualitative behavior of the resulting key boundary layer properties including the skin friction and three-dimensional displacement boundary layer thickness are then presented. The work is then further generalized to study the host flow pressure gradient effect on the disturbed boundary layer properties. Well-behaved solutions are obtained, and the disturbance velocities and shear stresses under both favorable or adverse pressure gradient of different intensities are presented and discussed.

2. Formulation of the Analysis

The following analysis considers a nominally two-dimensional incompressible laminar boundary layer flow over a wedge (i.e., Falkner-Skan flow) which is subjected to a weak free stream disturbance. The disturbance is spanwise-periodic, extends indefinitely far downstream, and has a spanwise wavelength that is constant but arbitrary. The governing equations are formulated in the orthogonal coordinate system shown in Figure 1 with the origin at the leading edge. We introduce the spanwise-sinusoidal disturbance as a small perturbation on a basic 2-D host flow U_o, V_o as follows:

$$u(x,y,z) = u_0(x,y) + \epsilon\, u_1(x,y)\, \cos(\frac{2\pi z}{\lambda}) + \ldots \quad (1)$$

$$v(x,y,z) = v_0(x,y) + \epsilon\, v_1(x,y)\, \cos(\frac{2\pi z}{\lambda}) + \ldots \quad (2)$$

$$w(x,y,z) = \epsilon\, w_1(x,y)\, \sin(\frac{2\pi z}{\lambda}) + \ldots \quad (3)$$

$$p(x,z) = p_0(x) + \epsilon\, p_1(x)\, \cos(\frac{2\pi z}{\lambda}) + \ldots \quad (4)$$

where $\epsilon << 1$. Substituting equation (3) into the 3-D governing Navier-Stokes flow equations, neglecting terms of second order and higher (i.e., assuming a weak disturbance field), and implementing the aforementioned assumptions, the first order perturbation equations for the U_1, V_1, and W_1 are:

$$\frac{\partial u_1}{\partial x} + \frac{\partial v_1}{\partial y} + \frac{2\pi}{\lambda} w_1 = 0 \quad (5)$$

$$u_0\frac{\partial u_1}{\partial x} + v_0\frac{\partial u_1}{\partial y} + u_1\frac{\partial u_0}{\partial x} + v_1\frac{\partial u_0}{\partial y} + \frac{1}{\rho}\frac{dp_1}{dx} = \nu\left[\frac{\partial^2 u_1}{\partial y^2} - \left(\frac{2\pi}{\lambda}\right)^2 u_1\right] \tag{6}$$

$$u_0\frac{\partial w_1}{\partial x} + v_0\frac{\partial w_1}{\partial y} - \frac{2\pi}{\lambda}\frac{p_1}{\rho} = \nu\left[\frac{\partial^2 w_1}{\partial y^2} - \left(\frac{2\pi}{\lambda}\right)^2 w_1\right] \tag{7}$$

subject to the boundary conditions

$$u_1 = v_1 = w_1 = 0 \quad @ \quad y = 0 \tag{8}$$

$$u_1 = 0, \quad w_1 = W_e \quad @ \quad y \to \infty \tag{9}$$

Similarly, the perturbation shear must vanish at the boundary layer edge:

$$\frac{\partial u_1}{\partial y} = \frac{\partial w_1}{\partial y} = \frac{\partial^2 u_1}{\partial y^2} = \frac{\partial^2 w_1}{\partial y^2} = 0 \quad @ \; y \to \infty \tag{10}$$

Notice that the outer-boundary conditions (9) further imply that $(\partial u_1/\partial x) = 0$ in the inviscid flow.

We next restrict our attention to the case where U_e takes a power law form $U_e = c(x/L)^m$ and consequently the host flow is of self-similar type (Falkner-Skan flow). Now this well-known solution is a self-similar one in terms of the stretched coordinate $\eta = y\sqrt{(m+1)U_e/\nu x}$ with stream function and velocity components

$$\psi_0 = \sqrt{\nu x U_e/(m+1)}\cdot f_0(\eta) \tag{11}$$

$$u_0 = U_e(x)\, f_0'(\eta) \tag{12}$$

$$v_0 = -\frac{1}{2}\left[(1+m)\frac{\nu U_e}{x}\right]^{\frac{1}{2}}\left[f_0(\eta) - \frac{1-m}{1+m}\eta f_0'(\eta)\right] \tag{13}$$

in which $f_0(\eta)$ is governed by the following ordinary differential equation split boundary value problem:

$$f_0''' + \frac{1}{2}f_0 f_0'' + \frac{m}{1+m}(1-f_0'^2) = 0 \tag{14a}$$

$$f_0(0) = f_0'(0) = 0 \quad ; \quad f_0'(\infty) \to 1 \qquad (14b) \qquad (14)$$

As suggested by the foregoing plus some preliminary study, we postulate the solution for disturbance velocity components in the following series expansion form:

$$\frac{w_1}{w_e} = \sum_{i=1}^{\infty} \xi^{(i-1)(1-m)} \left[\frac{2\pi V}{\lambda We}\right]^{i-1} G_i'(\eta) \qquad (15)$$

$$\frac{u_1}{U_e} = \sum_{i=1}^{\infty} \xi^{i(1-m)} \left[\frac{2\pi V}{\lambda We}\right]^{i-1} F_i'(\eta) \qquad (16)$$

where $\xi \equiv 2\pi X/\lambda$ is a rescaled non-dimensional streamwise distance. Then substituting equation (15) in (7) and setting the net coefficient of each power of ξ equal to zero, we obtain the following ordinary differential equations for the cross flow functions G_1, G_2... etc:

$$G_1''' + \tfrac{1}{2} f_0 G_1'' = 0 \qquad (17a)$$

$$G_2''' + \tfrac{1}{2} f_0 G_2'' + \tfrac{1}{1+m}(1 - G_1') = \left(\tfrac{1-m}{1+m}\right) f_0 G_2' \qquad (17b)$$

$$G_3''' + \tfrac{1}{2} f_0 G_3'' - \tfrac{1}{1+m} G_2' = 2\left(\tfrac{1-m}{1+m}\right) f_0 G_3' \qquad (17c)$$

$$\vdots \text{ etc.}$$

subject to the boundary conditions

$$G_i(0) = G_i'(0) = 0 \quad (i=1,2,3,\ldots) \qquad (18a)$$

$$G_1'(\infty) \to 1 \quad ; \quad G_j'(\infty) \to 0 \quad (j=2,3,4,\ldots) \qquad (18b)$$

Likewise from (6) and (16) the streamwise functions F_1, F_2, etc. are governed by

$$F_1''' + \tfrac{1}{2}[f_0F_1'' + (\tfrac{3-m}{1+m})f_0''F_1] + (\tfrac{1}{1+m})\, f_0''G_1 = f_0'F_1' \qquad (19a)$$

$$F_2''' + \tfrac{1}{2}[f_0F_2'' + (\tfrac{5-3m}{1+m})f_0''F_2] + (\tfrac{1}{1+m})\, f_0''G_2 - \tfrac{1}{1+m}F_1' = \tfrac{2}{1+m}f_0'F_2' \qquad (19b)$$

$$F_3''' + \tfrac{1}{2}[f_0F_3'' + (\tfrac{7-5m}{1+m})f_0''F_3] + (\tfrac{1}{1+m})\, f_0''G_3 - \tfrac{1}{1+m}F_2' = \tfrac{3-m}{1+m}f_0'F_3' \qquad (19c)$$

$$\vdots$$

$$\cdot\ etc.$$

with the boundary conditions

$$F_i(0) = F_i'(0) = 0 \quad ; \quad F_i'(\infty) \to 0 \quad (i=1,2,3,\ldots) \qquad (20)$$

These disturbance equations together with the host flow (14) have been simultaneously integrated numerically by the Runge-Kutta method [3]. Figures 2 and 3 show the typical results for the streamwise and cross-flow disturbance velocity functions $F_i'(\eta)$ and $G_i'(\eta)$, respectively, with different values of m. Additional overall properties of these solutions are summarized in Figure 4.

3. Discussion of Results

We observe from these results that the disturbance velocity functions and the corresponding wall shears are strongly amplified by an increasingly adverse pressure gradient. Furthermore, we expect that the first few terms of the series suffice to give numerical solutions with desired accuracy because with the increasing order (i) of the functions F_i, G_i, F_i, and G_i, their signs are alternating while the magnitudes of their peak amplitudes are decreasing for all values of m. Thus we see that an increasingly favorable pressure gradient decreases the sensitivity of the boundary layer properties to the 3-D disturbances whereas an adverse pressure gradient dramatically amplifies the disturbances. Moreover, from Figure 4 and the attendant skin friction relations (derived from the above analysis)

$$C_{f_x} = 2U_e\left[(1+m)\frac{\bar{U}_e}{R_{e_x}}\right]^{\frac{1}{2}}\left\{f_0''(0) + \epsilon\left[\sum_{i=1}^{\infty}\beta^{i-1}\xi^{i(1-m)}F_i''(0)\right]\cos\left(\frac{2\pi z}{\lambda}\right)\right\} \qquad (21)$$

$$C_{f_z} = 2\epsilon W_e\left[(1+m)\frac{\bar{U}_e}{R_{e_x}}\right]^{\frac{1}{2}}\left[\sum_{i=1}^{\infty}\beta^{i-1}\xi^{(i-1)(1-m)}G_i''(0)\right]\sin\left(\frac{2\pi z}{\lambda}\right) \qquad (22)$$

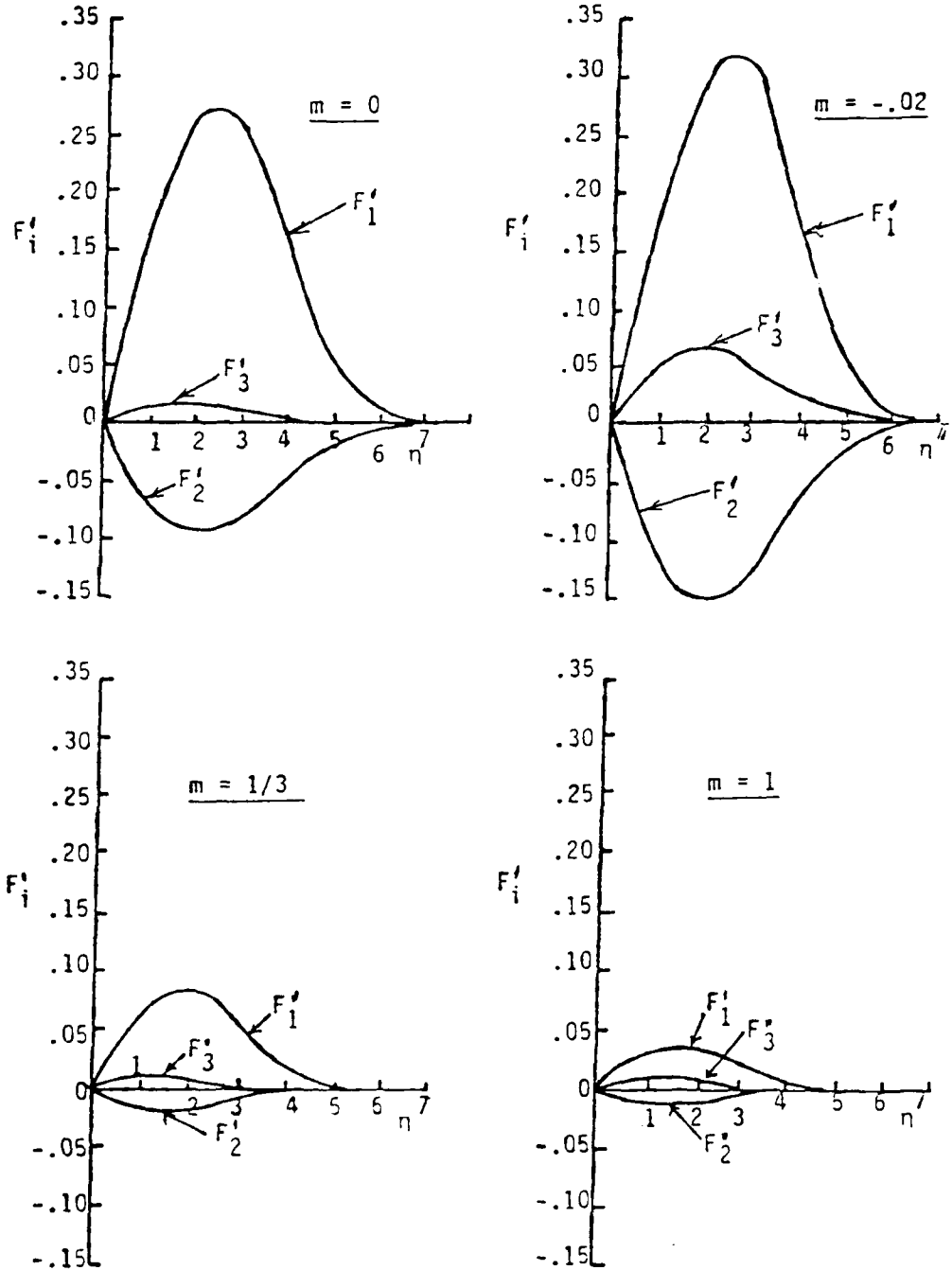

Fig. 2: Streamwise disturbance velocity functions in Falkner-Skan boundary-layer flow

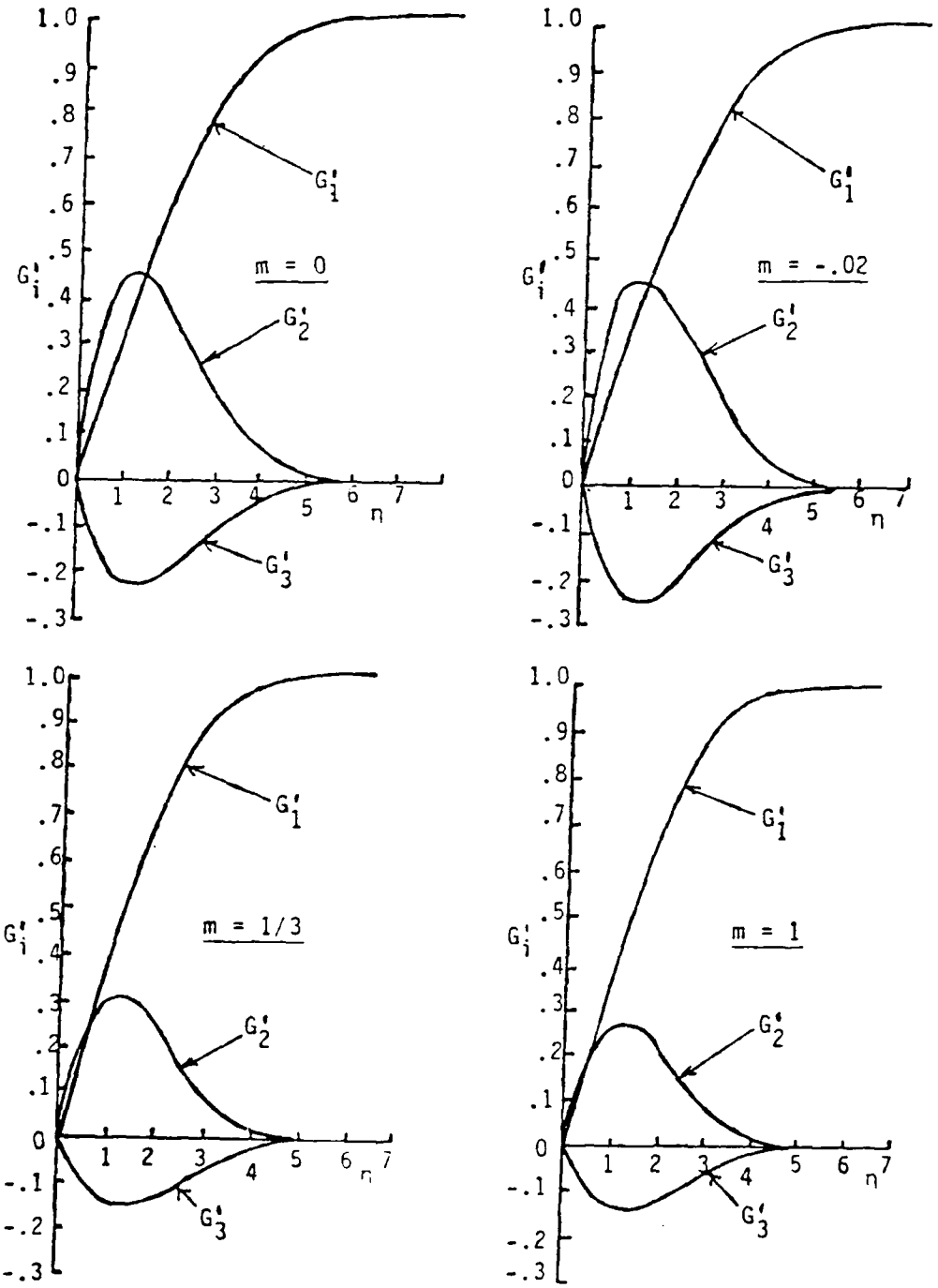

Fig. 3: Spanwise disturbance velocity functions in Falkner-Skan boundary-layer flow

Fig. 4: Host flow pressure gradient effect on flow properties

m	$f_o''(0)$	$[\eta_e - f_o(\eta_e)]$	$g'(o)$	$g(\eta_e)$	$f_1''(o)$	$f_1(\eta_e)$
1	.87160	.9150	.40521	2.966	.03411	.09186
1/3	.65563	1.143	.38299	2.995	.06775	.2260
0	.33504	1.692	.33488	3.207	.16739	.8587
-.02	.29229	1.807	.32615	3.266	.19210	1.039

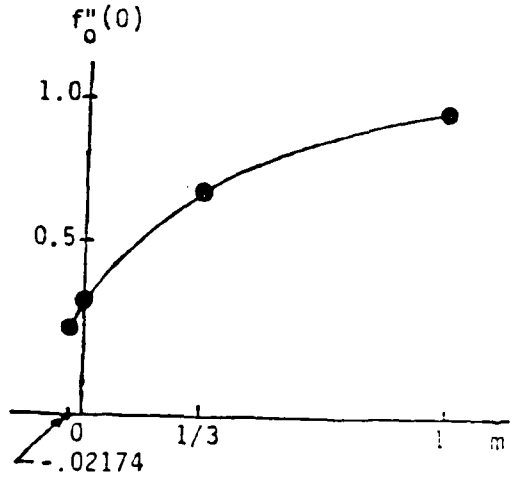

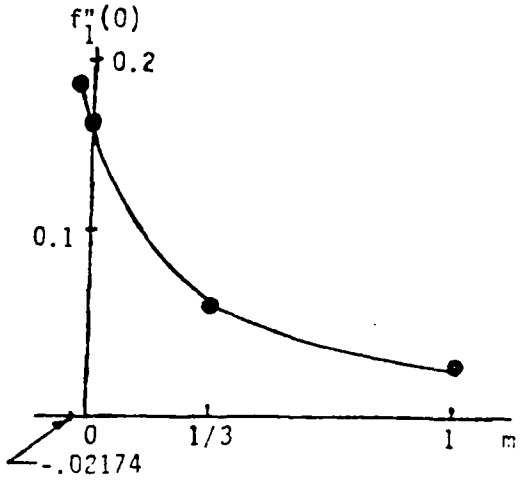

we see that an increasingly adverse pressure gradient decreases the basic term $f_0''(0)$ of C_{f_x} and, at the same time, increases its disturbance component $F_1''(0)$ and so may cause $C_{f_x} \to 0$ at spanwise stations $z = \lambda[(2n-1)/2]$, $n=1,2,3,..$. At these values of z, C_{f_z} also vanishes. Therefore, we expect a spanwise-periodic pattern of incipient separation as we intensify the adverse pressure gradient. In the full paper, the corresponding 3-D displacement thickness distribution will also be examined in detail.

Further study of our solution reveals that Fannelop's singularity in which the 3-D effect on u grows downstream without bound is, in fact, due to his neglect of the perturbation pressure and viscous z-derivative effects, whereas the complete solution including these terms takes a form of infinite series with Fannelop's solution as only the leading term. Thus, the perturbation pressure and the viscous z-derivatives correct and bound the leading term approximation which is otherwise singular. Furthermore, it is seen that these terms become more important for problems with smaller wavelength disturbances.

REFERENCES

1. Crow, S.C., "The Spanwise Perturbation of Two-Dimensional Boundary Layers." J. Appl. Mech., 24 (June 1965), 153-164.

2. Fannelop, T. K., "Effects of Streamwise Vortices on Laminar Boundary Layer Flow." ASME Trans. J. Appl. Mech., 35 (June 1968), 424-426.

3. Nachtsheim, P. R. and P. Swigert. "Satisfaction of Asymptotic Boundary Conditions in Numerical Solution of Systems of Nonlinear Equations of Boundary-Layer Type." NASA TN D-3004, October 1965.

4. Schlichting, H. Boundary Layer Theory, 6th ed. McGraw-Hill, New York, 1960.

5. White, F.M., Viscous Fluid Flow, McGraw Hill, New York, 1975.

6. Moore, F. K., "Three-Dimensional Boundary Layer Theory." Advances in Applied Mechanics, 4 (1956), 192-202.

AIAA'88

AIAA-88-3656

A Theory of Spanwise-Periodic Vortex Arrays Generated in the Boundary Layer Along a Rippled Plate

G.R. Inger and M. Konno
Iowa State University, Ames, Iowa

First National Fluid Dynamics Congress
July 25-28, 1988/Cincinnati, Ohio

"A THEORY OF SPANWISE-PERIODIC VORTEX ARRAYS GENERATED IN THE BOUNDARY LAYER ALONG A RIPPLED PLATE"

G.R. Inger* and M. Konno**

Iowa State University
Ames, Iowa

ABSTRACT

The generation of streamwise vorticity within the laminar boundary layer along a spanwise-rippled plate is theoretically investigated for the case where the ripple amplitude is small and grows linearly in the streamwise direction. Analytical solutions are obtained for the vortex-induced disturbance flow for arbitrary values of the spanwise wavelength to boundary layer thickness ratio. These are then used to examine the associated behavior of the 3-D skin friction and displacement thickness distributions.

NOMENCLATURE

$a(x)$	= peak amplitude of ripples
C_{f_x}, C_{f_z}	= component net skin friction coefficients
f_i	= streamwise similarity variables
g_i	= cross-flow similarity variables
L	= characteristic length
p	= static pressure
R_{e_x}, R_{e_λ}	= Reynolds numbers based on x and λ
u, v, w	= boundary layer velocity components
U, V, W	= outer inviscid flow velocity components
x, y, z	= streamwise, normal and cross-flow coordinates
δ_x^*, δ_z^*	= component displacement thicknessess
δ_{3D}^*	= 3-D displacement thickness
ϵ	= small expansion parameter
$\zeta_x, \zeta_y, \zeta_z$	= net vorticity components
η	= similarity coordinate
λ	= wavelength of ripples
μ	= coefficient of viscosity
ν	= kinetic viscosity coefficient
ξ	= nondimensional streamwise coordinate
ρ	= density
τ	= shear stress
ϕ	= harmonic potential
Φ	= amplitude of ϕ
ψ	= stream function
subscripts	
e	= poroperties at the boundary layer edge
w	= properties at the wall
∞	= freestream quantities
0	= undisturbed flow properties
1	= perturbed flow properties
inv	= wavy wall inviscid disturbance solution

*Glen Murphy Distinguished Professor, Dept. of Aerospace Engineering. Associate Fellow AIAA.

**Graduate Student, Dept. of Aerospace Engineering.

1. INTRODUCTION

The significant effect of streamwise-vortex arrays on a host boundary layer is well known. In particular, the resulting enhanced mixing rate of the combined flow ("vortex-generator" effect) is of great practical interest in conjunction with both external aerodynamic flow fields and those within turbomachinery devices.

Recently, Werle and his co-workers [1] have drawn attention to the favorable effects occurring from the use of a spanwise-periodic surface pattern on an airfoil to generate such vortex arrays and have reported on experimental observations of the resulting enhanced mixing and separation effects in the wake downstream of the airfoil. In the present paper, we give a theoretical analysis of such an array for the simplified case of attached incompressible laminar boundary layer flow along a slightly spanwise rippled flat plate (see Fig. 1). Our main focus is to illuminate the physics of the streamwise vortex generation and its three-dimensional influence on the flow within the highly viscous region near the surface.

2. FORMULATION OF THE ANALYSIS

Our theoretical treatment rests on the following assumptions:

- Small-amplitude surface ripples that grow linearly with streamwise distance: $y_w = \epsilon a \sin\left(\frac{2\pi z}{\lambda}\right)$ with $a = x$ and ϵ a given non-dimensional small parameter.
- Arbitrary given spanwise wavelength λ
- High Reynolds number laminar flow
- Steady incompressible flow
- Resulting disturbance vortices extend infinitely far downstream.

The analytical approach is a perturbation method, analogous to that used by the Junior author in a similar study of freestream vortex-array effects [2], wherein the flow properties are expressed as small spanwise-periodic disturbances upon the basic Blasius boundary-layer:

$$p(x,z) = p_\infty + \epsilon p_1(x)\sin\left(\frac{2\pi z}{\lambda}\right) + \cdots \quad (1)$$

$$u(x,y,z) = u_0(x,y) + \epsilon u_1(x,y)\sin\left(\frac{2\pi z}{\lambda}\right) + \cdots \quad (2)$$

$$v(x,y,z) = v_0(x,y) + \epsilon v_1(x,y)\sin\left(\frac{2\pi z}{\lambda}\right) + \cdots \quad (3)$$

$$w(x,y,z) = \epsilon w_1(x,y)\cos\left(\frac{2\pi z}{\lambda}\right) - \cdots (sidewash) \quad (4)$$

where u_0 and v_0 belong to the Blasius flow. Substitution into the basic governing Navier-Stokes equations under the high Reynolds number conditions of negligible $\partial p/\partial y$ and $\mu\,(\partial^2 / \partial\, x^2)$ effects within the boundary layer, retaining only the leading order ϵ approximation for the wavyness-induced disturbances, and then subtracting out the basic undisturbed flow relations yield appropriate sets of differential equations governing the disturbance distribution functions p_1, u_1, v_1, and w_1 (see 2.2 below). These are to be solved subject to the outer boundary conditions that u and w at the boundary layer edge approach values given by their near-wall inviscid solution counterparts to the same rippled wall problem, while along the impermeable surface they are subject to the no slip condition, giving to order ϵ that

$$v_1(x,0) = 0 \quad (5)$$

$$u_1(x,0) \simeq -x\frac{\partial u_0}{\partial y}(x,0) \quad (6)$$

$$w_1(x,0) \simeq 0 \quad (7)$$

2.1 Inviscid Disturbance Solution

Irrotational inviscid (potential) flow past the rippled-type of plate shown in Fig. 1 exhibits in itself a non-trivial disturbance solution. This is necessarily governed, in general, by a harmonic disturbance potential $\phi_1(x,y,z)$ such that $u - U_0 = \partial\phi_1/\partial x$ and $w = \partial\phi_1/\partial z$ vanish in the uniform mainstream U_0 far from the plate while on the surface satisfying the inviscid impermeability condition that $V_1(x,0) = -U_0$. In view of Eqs. (1)-(4), ϕ_1 is further postulated to have the spanwise-periodic form $\phi_1 = \epsilon U_0 \Phi(x,y)\sin\left(\frac{2\pi z}{\lambda}\right)$ whereupon Φ is governed by the Helmholtz equation

$$\frac{\partial^2\Phi}{\partial x^2} + \frac{\partial^2\Phi}{\partial y^2} = \left(\frac{2\pi}{\lambda}\right)^2 \Phi \quad (8)$$

subject to the conditions that Φ vanish for large (x^2+y^2) while $\frac{\partial\Phi}{\partial y}(x,0) = 1$.

Now some preliminary study reveals that a solution of Eq. (8), having the desired property that u_1 (and hence $\partial\Phi/\partial x$) vanish for an assumed infinite downstream length of ripples, is given by the separation of variables form[*]

$$\Phi = -\frac{\lambda}{2\pi}\exp\left(-\frac{\lambda y}{2\pi}\right) \quad (9)$$

From this, we then obtain the inviscid sidewash disturbance velocity at the wall of the present problem (which is the outer boundary value for the underlying boundary layer behavior) as

$$w_{1_{out}}(x, y=0) = \frac{\partial\phi_1}{\partial z}(x,0) = -U_0 \quad (10)$$

2.2 Viscous Boundary Layer Disturbance Field

The perturbation functions u_1, v_1 and w_1 of Eqs. (1)-(4) within the boundary layer are governed by the following set of equations:

$$\frac{\partial u_1}{\partial x} + \frac{\partial v_1}{\partial y} + \left(\frac{2\pi}{\lambda}\right) w_1 = 0 \quad (11)$$

$$u_0\frac{\partial u_1}{\partial x} + v_0\frac{\partial u_1}{\partial y} + u_1\frac{\partial u_0}{\partial x} + v_1\frac{\partial u_0}{\partial y} + \frac{1}{\rho}\frac{\partial p_1}{\partial x} = \nu\left[\frac{\partial^2 u_1}{\partial y^2} - \left(\frac{2\pi}{\lambda}\right)^2 u_1\right] \quad (12)$$

$$u_0\frac{\partial w_1}{\partial x} + v_0\frac{\partial w_1}{\partial y} + \frac{2\pi}{\lambda}\frac{p_1}{\rho} = \nu\left[\frac{\partial^2 w_1}{\partial y^2} - \left(\frac{2\pi}{\lambda}\right)^2 w_1\right] \quad (13)$$

These equations are to be solved subject to the wall boundary conditions given by Eqs. (5)-(7) with a non-zero $\frac{\partial u_0}{\partial y}(x,0) = \tau_{w_0}/\mu_w$, plus the outer inviscid flow matching conditions that

$$u_1(x, y\to\infty) = 0 \quad (14)$$

$$w_1(x, y\to\infty) = W_{1_{out}}(x,0) = -U_0 \quad (15)$$

corresponding to the vanishing disturbance (as well as basic) flow shear stress conditions

$$\frac{\partial u_1}{\partial y}(x, y\to\infty) = \frac{\partial w_1}{\partial y}(x, y\to\infty) = 0 \quad (16)$$

The attendant pressure perturbation is determined by observing, from conditions (14)-(16) plus Eq. (13), that the disturbance pressure is directly associated with the cross flow viscous shear term $\sim \mu(\partial^2 w/\partial x^2)$ and equal to the x independent constant non-dimensional value

$$\left(\frac{p_1}{\rho U_{0_\infty}^2}\right) = \frac{\mu}{\rho U_{0_\infty}\lambda} \equiv R_{\lambda}^{-1} \quad (17)$$

This value is seen to be very small for high Reynolds number flows except with small scale surface ripple wavelengths. In any case, it does not contribute to the x-momentum Eq. (12) because $\partial p/\partial x \equiv 0$.

Since the basic host flow is a self-similar one (the Blasius solution), it proves convenient to reformulate the foregoing disturbance flow problem in terms of the appropriate similarity coordinate $\eta = y(U_{0_\infty}/\nu x)^{1/2}$. The basic flow stream function ψ_0 (such that $u_0 \equiv \partial\psi_0/\partial y$, $v_0 \equiv -\partial\psi_0/\partial x$) can then be expressed in the form $\psi_0 = (\nu U_{0_\infty} x)^{1/2} f_0(\eta)$ where f_0 is governed by Blasius's well-known ordinary differential equation,

$$f_0''' + \frac{1}{2} f_0 f_0'' = 0 \quad (18)$$

where $()' \equiv d()/d\eta$ and f_0 satisfies the split boundary conditions $f_0(0) = f_0'(0) = 0$, $f_0'(\infty) \to 1$ with $f_0'' \to 0$.

[*] This solution excludes a small streamwise leading edge region $x \lesssim (\lambda/2\pi)$ that is also excluded by our neglect of viscous x-derivative terms compared to those of z-derivative in the underlying boundary layer region.

Now, some preliminary study reveals that the corresponding perturbation velocities in the present problem must behave for small x as $u_1 \sim x^{1/2}F(\eta)$, $w_1 \sim G(\eta)$ where F and G are functions of η only; accordingly, to cover the entire range of x we postulate solutions in the form of the following series:

$$u_1 = \frac{U_{0_e} R_{e_1}}{2\pi}\left[\xi^{1/2} f_1'(\eta) + \sum_{i=2}^{\infty} \xi^{i-1} f_i'(\eta)\right] \quad (19)$$

$$w_1 = -U_{0_e} \sum_{i=1}^{\infty} \xi^{i-1} g_i'(\eta) \quad (20)$$

where $\xi = x/L$ is a rescaled streamwise distance in terms of a conveniently-chosen characteristic length L specified below, and $f_i(\eta)$ and $g_i(\eta)$ are governed by suitable ordinary differential equations. Further, we introduce a 3-D disturbance stream function ψ_1 such that

$$u_1 = \frac{\partial \psi_1}{\partial y} \quad (21)$$

$$v_1 = -\frac{\partial \psi_1}{\partial x} - \frac{2\pi}{\lambda}\int_0^y w_1(x, Y)dY \quad (22)$$

(thereby satisfying Eq. (11)) and postulate for it the form

$$\psi_1 = (\nu U_{0_e} x)^{1/2} R_{e_1}\left[\xi^{1/2} f_1(\eta) + \sum_{i=1}^{\infty} \xi^{i-1} f_i(\eta)\right] \quad (23)$$

Then substituting expressions (19)-(23) into Equations (12) and (13) after transformation from (x, y) to (ξ, η), equating to zero the net coefficients of each power of ξ, and choosing $L \equiv (\lambda/2\pi)^2 U_{0_e}/\nu$ in order to obtain an universal form of the equations, we ultimately arrive at the following set of Equations governing the g_i and f_i, respectively:

$$g_1''' + \frac{1}{2} f_0 g_1'' = 0 \quad (24)$$

$$g_2''' + \frac{1}{2} f_0 g_2'' - f_0' g_2' = g_1' - 1 \quad (25)$$

$$g_3''' + \frac{1}{2} f_0 g_3'' - 2 f_0' g_3' = g_2' \quad (26)$$

$$\vdots$$

$$g_i''' + \frac{1}{2} f_0 g_i'' - (i-1) f_0' g_i' = g_{i-1}' \quad (27)$$

and

$$f_1''' + f_1 f_0'' + \frac{1}{2} f_1'' f_0 - \frac{1}{2} f_0' f_1' = 0 \quad (28)$$

$$f_2''' + \frac{1}{2}(f_0 f_2'' + 3 f_0'' f_2) - f_0' f_2' + f_0'' g_1 = 0 \quad (29)$$

$$f_3''' + \frac{1}{2}(f_0 f_3'' + 5 f_0'' f_3) - 2 f_0' f_3' = f_1' - f_0'' g_2 \quad (30)$$

$$\vdots$$

$$f_i''' + \frac{1}{2}\left[f_0 f_i'' + (2i-1) f_0'' f_i\right] - (i-1) f_0' f_i' = f_{i-2}' - f_0'' g_{i-1} \quad (31)$$

The corresponding boundary conditions derive from Eqs. (5)-(7) and (14)-(15) and yield:

$$g_i(0) = g_i'(0) = 0 \quad (32)$$

$$g_1'(\infty) \to 1, \; g_{i-1}'(\infty) \to 0 \quad (33)$$

and

$$f_1'(0) = -f_0''(0) \quad (34)$$

$$f_i(0) = f_{i-1}'(0) = 0 \quad (35)$$

$$f_i'(\infty) = 0 \quad (36)$$

where $i = 1, 2, 3, \ldots$.

The foregoing equations constitute a system of coupled linear ordinary differential equations with split boundary conditions that can be readily solved numerically by a standard shooting technique combined with the Runge-Kutta integration method[3]. Before proceeding to a presentation and discussion of the results, an important general feature of Eqs. (24)-(27) governing the cross flow should be noted: the non-homogeneous terms on the right hand sides derive entirely from the viscous $\mu(\partial^2 u, w/\partial z^2)$ effect and its associated small pressure disturbance (Eq. 17), and would otherwise be zero if these effects were neglected a priori. Since the boundary conditions on g_i for $i \geq 2$ are completely homogeneous, this in turn means that all the $g_i(\eta)$ would necessarily be identically zero as well. Thus, all the terms in series (20) that involve a non-zero power of ξ physically represent the entire cumulative downstream influence of this small viscous cross flow effect. Likewise, all the streamwise disturbance functions $f_i(\eta)$ for $i \geq 3$ [i.e, the right hand sides of Eqs. (30) and beyond] derive solely from including the effects of the $\mu(\partial^2 u/\partial z^2)$ term and would otherwise be zero if this effect were neglected. In this later case, only the first two terms of the series (19) would remain; these express the leading approximation to the dual physical effects of (a) the streamwise velocity disturbance due to the surface ripple effect via the no-slip condition at the wall [this being $\sim \xi^{1/2}$ and hence the most dominant effect], followed by (b) the disturbance within the boundary layer caused by the overlying inviscid cross-flow perturbation induced by the ripples, growing like ξ and hence taking effect further downstream.

3. RESULTS AND DISCUSSION

3.1 Disturbance Velocities and Skin Friction

Numerical results for the first four ($i = 1, 2, 3$ and 4) disturbance velocity functions $g_i'(\eta)$ and $f_i'(\eta)$ across the boundary layer are presented in Figures 2 and 3, respectively; the corresponding shear stress distributions $g_i''(\eta)$ and $f_i''(\eta)$ are illustrated in Figs. 4 and 5. Beyond $i = 2$, it is seen that the maximum value of these perturbations decreases in magnitude and alternates in sign with increasing i, implying that the higher order terms in ξ contribute to the series solutions (19) and (20) in only a small and cancelling way at larger downstream distances. It should be noted that it becomes

increasingly difficult to compute the decreasing values of the functions at larger i because even a small round off error grows relatively large with respect to the very small target value.

The special values $f_i''(0)$ and $g_i''(0)$, related to the streamwise and cross-shear disturbances on the surface, are tabulated in Table I up to $i = 4$. From these, the physical skin friction components can be reconstructed from the present similarity series solution, as follows. For the streamwise skin friction coefficient, we have $C_{f_x} \equiv 2\mu(\partial u/\partial y)_w/(\rho U_\infty^2)$ which via the similarity transformation and Eq. (19) leads to the final expression

$$C_{f_x} R_{x_0}^{1/2} = 2f_0''(0) - \frac{\epsilon R_{x_0}}{2\pi}\left[\xi^{1/2} f_1'(0) + \sum_{i=2}^{\infty} \xi^{i-1} f_i''(0)\right] \sin\left(\frac{2\pi x}{\lambda}\right) \qquad (37)$$

where $f_0''(0) = .3321$ pertains to the undisturbed flat plate boundary layer. The corresponding spanwise skin friction component $C_{f_z} \equiv 2\mu(\partial w/\partial y)_w/(\rho U_\infty^2)$ likewise comes out to be

$$C_{f_z} R_{x_0}^{1/2} = -\epsilon\left[\sum_{i=1}^{\infty} \xi^{i-1} g_i''(0)\right] \cos\left(\frac{2\pi x}{\lambda}\right) \qquad (38)$$

Several interesting conclusions emerge from an inspection of Eqs. (37) and (38). First, since $f_1''(0)$ is zero while $g_1''(0)$ is not (Table I), it is seen that the leading-term approximation for the rippled wall effect at small ξ does <u>not</u> contribute to the streamwise shear stress C_{f_x} but only to the cross flow component; the <u>next</u> term ($i = 2$) associated with the <u>inviscid</u> cross flow disturbance produced by the ripples, however, does influence C_{f_x}. Second, we can infer from Eq. (37) that the ripples will hasten the onset of streamwise separation $C_{f_x} \to 0$ at those spanwise stations where the perturbation contribution on the right hand side has a maximum negative value. Since $f_2''(0)$, $g_1''(0)$ and $g_2''(0)$ are all positive (Table I), this will occur in the leading approximation at stations where $(2\pi x/\lambda) = 3\pi/2, 7\pi/2, \ldots$; by Eq. (38) and Fig. 6, these correspond to spanwise locations that are troughs in the ripples <u>and</u> where also the cross flow shear exactly vanishes.

3.2 Streamwise Vorticity Generation

One of the important features of the present theory is the prediction from first principles of how streamwise vorticity ζ_x is generated by the spanwise ripple effect acting deep within the viscous boundary layer. This can be determined from the foregoing analysis by developing the basic relationship for ζ_x in terms of the above similarity-series solutions.

Now it can be shown from an examination of the general Navier-Stokes equations that, consistent with the high Reynolds number boundary layer model equations adopted in the present study (specifically, Eqs. 11-13), we should also employ the following boundary layer-approximations to the corresponding vorticity components: $\zeta_x \simeq \partial u/\partial y$, $\zeta_y \simeq -\partial u/\partial z$ and $\zeta_z \simeq -\partial w/\partial y$. Focusing on the later streamwise component as the one of primary interest here, we thus get from Eqs. (4) and (20) that

$$\zeta_x R_{x_0}^{-1/2} \simeq \frac{U_{e_0}}{x}\epsilon \cos\left(\frac{2\pi x}{\lambda}\right)\left[\sum_{i=1}^{\infty} \xi^{i-1} g_i''(\eta)\right] \qquad (39)$$

In view of the properties of the functions $g_i''(\eta)$ shown in Fig. 4, Eq. (39) predicts as expected that the streamwise vorticity generated by the surface ripples is a maximum at the wall. Consistent with our original assumption that the inviscid velocity disturbance field caused by the ripples is irrotational, this equation also correctly yields vanishing vorticity outside the boundary layer since all the $g_i''(0) \to 0$ as $\eta \to \infty$. Finally, we note that since the $g_i''(0)$ are positive for $i \leq 2$, the present theory predicts in the leading approximation that the largest streamwise vorticity generation occurs at the lateral stations of maximum spanwise slope and cross-flow shear stress (Fig. 6) as one would expect on physical grounds.

3.3 Displacement Thickness Distribution

The three dimensional perturbation field due to the spanwise ripples also alters the displacement thickness distribution along the plate and hence the effective body seen by the inviscid flow. Since this property may be of interest in subsequent studies of high speed boundary layers, we conclude by examining it in the present problem to obtain some insight as to the interactive "vortex-generator effect" on the inviscid flow.

Now the general 3-D displacement thickness distribution $\delta_{3D}^*(x,z)$ is defined by the first order partial differential equation[4]

$$\frac{\partial}{\partial x}\left[U_e(\delta_{3D}^* - \delta_x^*)\right] + \frac{\partial}{\partial z}\left[W_e(\delta_{3D}^* - \delta_z^*)\right] = 0 \qquad (40)$$

where δ_x^* and δ_z^* are the streamwise and cross-flow displacement thicknesses defined by

$$\delta_x^* = \int_{y|_{w=0}}^{\infty}\left(1 - \frac{u}{U_e}\right)dy = \int_{y_w}^{\infty}\left(1 - \frac{u}{U_e}\right)dy \qquad (41)$$

and

$$\delta_z^* = \int_{y|_{w=0}}^{\infty}\left(1 - \frac{w}{W_e}\right)dy = \int_{y_w}^{\infty}\left(1 - \frac{w}{W_e}\right)dy \qquad (42)$$

Upon substituting the expressions for w, u and y_w from the above analysis, expanding the lower limits of Eqs. (41)-(42) in a Taylor series about $y = 0$, retaining only the order ϵ 3-D effects, and expressing results in terms of our similarity variable formulation, we obtain the following expressions:

$$(\delta_x^*/x)\, R_{x_0}^{1/2} = \alpha_0 - \epsilon \sin\left(\frac{2\pi x}{\lambda}\right) \times \left\{R_{x_0} \lim_{\eta\to\infty}\left[\xi^{1/2} f_1(\eta) + \sum_{i=2}^{\infty} \xi^{i-1} f_i(\eta)\right] + R_{x_0}^{1/2}\right\} \qquad (43)$$

$$(\delta_z^*/x)\, R_{x_0}^{1/2} = \alpha_1 + \lim_{\eta\to\infty}\left\{\sum_{i=2}^{\infty} \xi^{i-1} g_i(\eta)\right\} + \epsilon R_{x_0}^{1/2} \sin\left(\frac{2\pi x}{\lambda}\right) \qquad (44)$$

where the various numerical values of the constants $\alpha_0 \equiv \lim_{\eta \to \infty} [\eta - f_0(\eta)]$, $\alpha_1 \equiv \lim_{\eta \to \infty} [\eta - g_1(\eta)]$, $g_i(\infty)$ and $f_i(\infty)$ are given in Table I.

Now consistent with the perturbation approach of the present analysis, the solution of Eq. (40) takes the form $\delta^*_{3D} \simeq \delta^*_0(x) + \epsilon\delta^*_1(x)\sin(2\pi z/\lambda)$; after some elementary calculus, the following results are obtained from Eqs. (43) and (44):

$$(\delta^*_0/x)\, R^{1/2}_{x_0} = \alpha_0 \tag{45}$$

$$(\delta^*_1/x)\, R^{1/2}_{x_0} = -R^{1/2}_{x_0} - R_{x_\lambda}\left\{\xi^{1/2} \lim_{\eta \to \infty} f_1(\eta) + \lim_{\eta \to \infty} \sum_{i=2}^{\infty} \left[\xi^i g_i(\eta)/(i - \tfrac{1}{2}) + \xi^{i-1} f_i(\eta)\right]\right\} \tag{46}$$

It is interesting to note that the g_1 term, although contributing to δ^*_1, does <u>not</u> ultimately appear in the δ^*_1 expression; this is because the $\lim_{\eta \to \infty}[\eta - g_1(\eta)]$ is canceled in Eq. (40) by the $\lim_{\eta \to \infty}[\eta - f_0(\eta)]$ term in δ^*_0 (see Table I). It can be seen from Eq. (46) that the perturbation of the viscous displacement effect due to the surface ripples (in the leading approximation) is 180° out of phase with the wall ripples and so causes a local increase in δ^* in the surface valleys, while a corresponding thinning of the boundary layer occurs in the same ripple pattern location as does the minimum streamwise skin friction.

4. CONCLUDING REMARKS

The present study has shown that it is possible to construct a basic analysis of how small amplitude spanwise-periodic ripples on a surface generate streamwise vorticity in an overlying laminar boundary layer flow. The results should prove usefull as an intreptive guide, and perhaps also as an upstream starting solutions, in the numerical treatment of the more general nonlinear problem associated with larger amplitude disturbances.

The compressible-flow counterpart of the present problem, including especially the 3-D heat transfer disturbances associated with these streamwise vortices, would be of considerable practical interest as a follow-on investigation.

ACKNOWLEDGEMENT

This work was carried out under the support of Grant 85-0357A from the U.S. Air Force Office of Scientific Research.

REFERENCES

[1]Werle, M.J., Paterson, R.W. and Presz, R.M., "Flow Structure in a Periodic Axial Vortex Array," AIAA Paper 87-0610, 1987.

[2]Konno, M. "A Theoretical Study of Spanwise-Periodic Disturbances in Falkner-Skan Boundary-Layer Flows," M.S. Thesis, Iowa State University, 1987.

[3]Nachtsheim, P.R. and Swigert, P. "Statisfaction of Asymptotic Boundary Conditions in Numerical Solution of Systems of Nonlinear Equations of Boundary-Layer Type," NASA TN D-3004, 1965.

[4]Moore, F.K. "Three-Dimensional Boundary Layer Theory," Advances in Applied Mechanics, vol 4, 1956.

TABLE I: Numerical Results of Key Properties

i	$f_i''(0)$	$g_i''(0)$	$\lim_{\eta \to \infty} f_i(\eta)$	$\lim_{\eta \to \infty} g_i(\eta)$
1	0.0000	0.3321	−0.9954	———
2	0.1661	0.8756	0.8492	1.090
3	0.6028	−0.3327	1.558	−0.5782
4	−0.2343	0.1374	−0.8598	0.08261

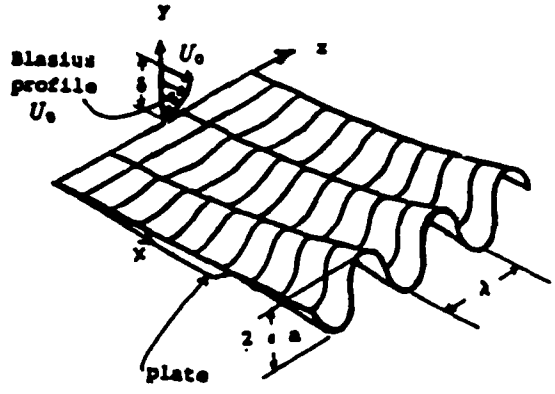

Fig. 1: Schematic of the Rippled Plate Flow Problem

Fig. 2:
Cross-flow disturbance velocity functions

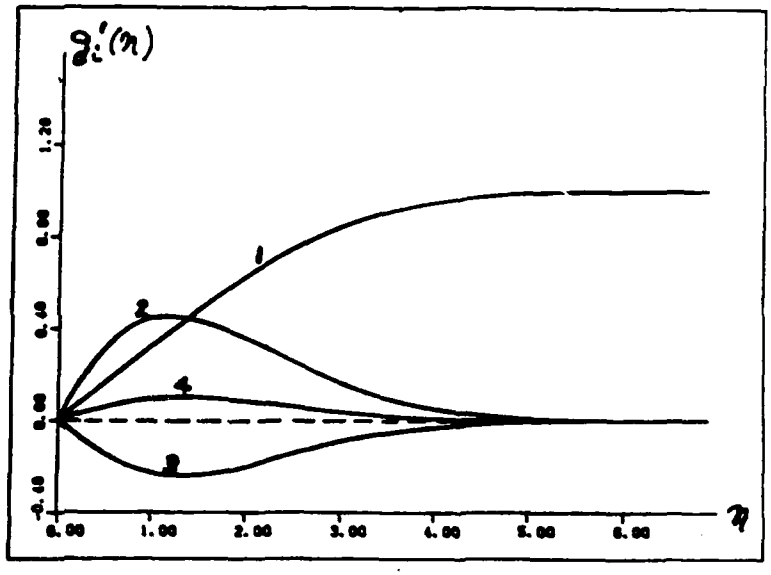

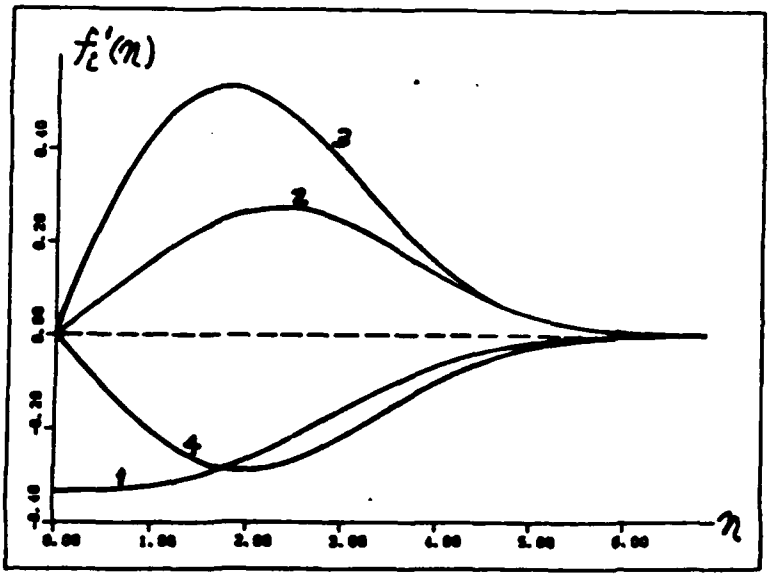

Fig. 3:
Streamwise disturbance velocity functions

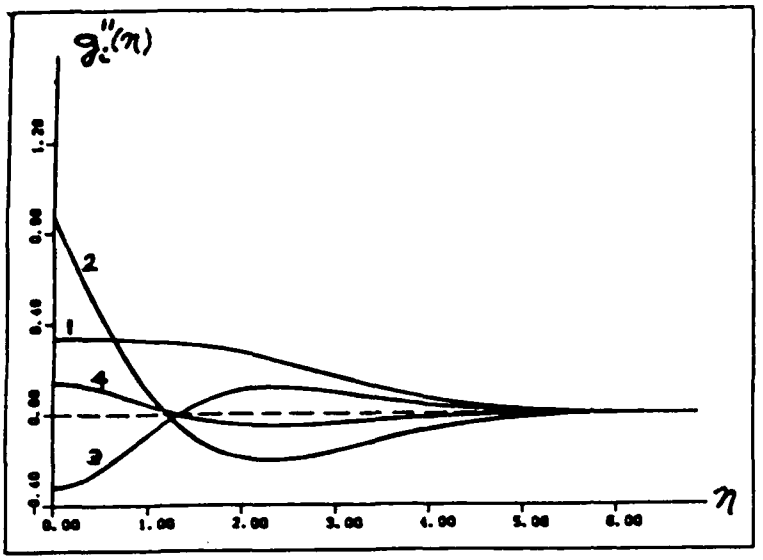

Fig. 4:
Cross-flow disturbance shear functions

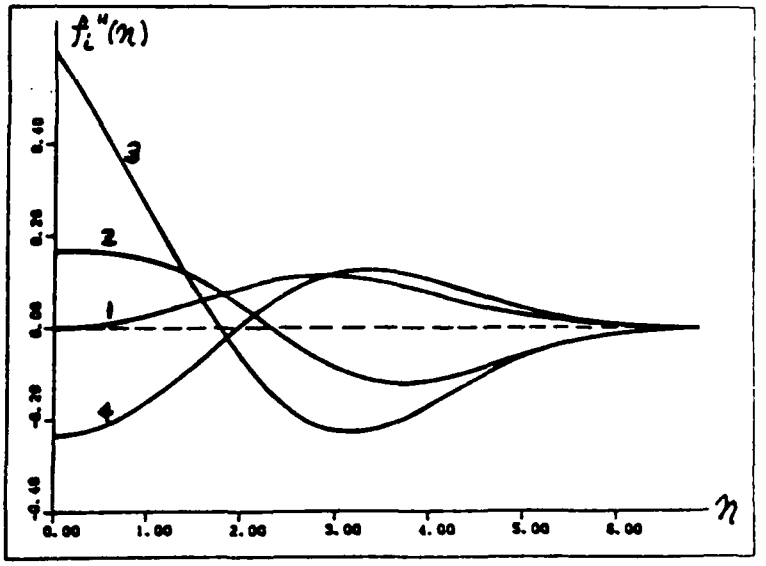

Fig. 5:
Streamwise disturbance shear functions

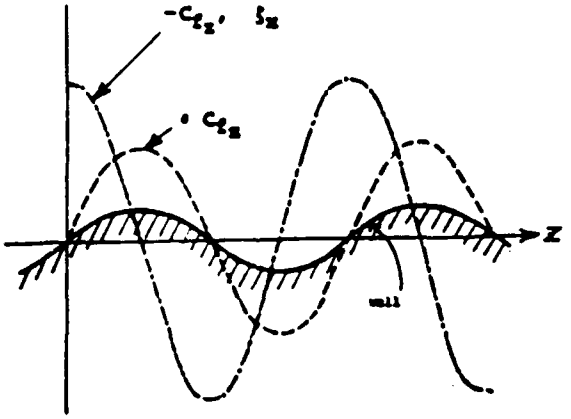

Fig. 6: Spanwise Distribution of Skin Friction and Streamwise Vorticity

AIAA'88

AIAA-88-3581

The Role of Law of the Wall/Wake Modeling in Validating Shock-Boundary Layer Interaction Predictions

G.R. Inger
Iowa State University, Ames, Iowa

First National Fluid Dynamics Congress
July 25-28, 1988/Cincinnati, Ohio

"THE ROLE OF LAW OF THE WALL/WAKE MODELING IN VALIDATING SHOCK-BOUNDARY LAYER INTERACTION PREDICTIONS"

G. R. Inger*
Department of Aerospace Engineering
Iowa State University

ABSTRACT

The treatment of turbulence effects on supersonic shock/turbulent boundary layer interaction is addressed within the context of a triple deck approach valid for arbitrary practical Reynolds numbers $10^3 < Re_\delta \leq 10^{10}$. The modeling of the eddy viscosity and basic turbulent boundary profile effects in each deck is examined in detail using Law of the Wall/Law of the Wake concepts as the foundation. Results of parametric studies are then given, showing how each of these turbulence model aspects influences the important interaction zone property of upstream influence.

Nomenclature

a	speed of sound
A	Van Driest wall turbulence damping parameter
C_f	skin friction coefficient $\left(2\tau_w/\rho_{e_o} U^2_{e_o}\right)$
H, H_i	shape factor δ^*/θ^*, incompressible shape factor
$H(T)$	interactive turbulence effect on inner deck thickness
ℓ_u	upstream influence distance
M	Mach number
p, p'	static pressure, static pressure perturbation $(p - p_{e_o})$
ΔP	pressure jump across undisturbed incident shock
Re_ℓ, Re_δ	Reynolds numbers based on length and boundary layer thickness,
$S(T)$	interactive turbulent effect on skin friction perturbation
T	absolute temperature
$\mathcal{T}$	basic interactive wall-turbulence parameter
u', v'	streamwise and vertical interactive disturbance velocity components
U_o	undisturbed incoming boundary layer profile
x, y	streamwise and vertical coordinates, respecively
y_{weff}	effective wall shift (displacement height of inner deck) seen by interactive inviscid flow
β	$\sqrt{M_1^2 - 1}$
γ	specific heat ratio
δ	boundary layer thickness
δ^*	boundary layer displacement thickness
δ_{SL}	inner deck sublayer thickness
μ, ν	ordinary and kinematic coefficients of viscosity, respectively
ν_t	turbulent kinematic eddy viscosity
ω	viscosity-temperature dependence exponent $(\mu \sim T^\omega)$
ρ	density
θ^*	boundary layer momentum thickness
τ_w	shear stress
τ'_w	interactive perturbation of shear stress

Subscripts

AD	adiabatic wall conditions
1	undisturbed inviscid values ahead of incident shock
e	conditions at the boundary layer edge
inv	inviscid disturbance solution value
o	value pertaining to the undisturbed incoming boundary layer profile
w	conditions at the surface ("wall")

1. INTRODUCTION

Shock/Boundary Layer Interaction is a significant feature of the flow fields around control surfaces and within air-breathing engine inlets on supersonic/hypersonic aerodynamic vehicles. Experimental validation of CFD codes designed to accurately predict the essential properties of such interactions is therefore of practical importance. In particular, it is very desirable to know the sensitivity of these properties to the basic parameters that govern the turbulent structure of the incoming turbulent boundary layer (upon which the subsequent interaction depends). While the influence of various turbulence models on different types of aerodynamic flow field calculations has been extensively studied, especially under separated flow conditions (see, e.g., Ref. 1), there remains the need for a systematic study of the shock/boundary layer interaction problem per se within the context of the Law of the Wall/Wake concept that is widely employed by experimentalists to characterize the turbulent boundary layer. The present paper addresses this question for the case of two-dimensional supersonic non-separating shock or compression corner-generated interactions on adiabatic walls.

Since it has been clearly shown by the late R.T. Davis and others that all successful CFD treatments of such interactions must recognize the inherent triple-deck structure of the interaction zone (Fig. 1), our approach is formulated in terms of this structure using eddy viscosity concepts. Because it has proven applicable to a very wide range of Reynolds numbers and adaptable to practical flow field calcuation schemes, we employ for this purpose the non-asymptotic version of this triple-deck theory due to Inger.[2] The modeling of the eddy viscosity and mean velocity profile effects in each deck is then examined using the Law of the Wall/Wake framework as the foundation.

*Glenn Murphy Distinguished Professor, Department of Aerospace Engineering. Associate Fellow, AIAA.

2. RATIONALE OF THE TRIPLE DECK APPROACH

Since it is the foundational framework used to address the various turbulence-modeling issues, a brief outline of the triple-deck approach and the advantages of its non-asymptotic version will first be given. We consider small disturbances of an arbitrary incoming turbulent boundary layer due to a weak external shock and examine the detailed perturbation field within the layer. At high Reynolds numbers it has been established that the local interaction disturbance field in the neighborhood of the impinging shock organizes itself into three basic layered-regions or "decks" (Figure 1): 1) an outer region of potential inviscid flow above the boundary layer, which contains the incident shock and interactive wave systems; 2) an intermediate deck of rotational-inviscid disturbance flow occupying the outer 90% or more of the incoming boundary layer thickness; 3) an inner sublayer adjacent to the wall containing both turbulent and laminar shear stress disturbances, which accounts for the interactive skin friction perturbations and hence any possible incipient separation plus most of the upstream influence of the interaction. The "forcing function" of the problem here is thus impressed by the outer deck upon the boundary layer; the middle deck couples this to the response of the inner deck but in so doing can itself modify the disturbance field to some extent, while the slow viscous flow in the thin inner deck reacts very strongly to the pressure gradient disturbances imposed by these overlying decks. This general triple deck structure is supported by a large body of experimental and theoretical studies.[2]

Concerning the importance of the inner shear disturbance deck and the accuracy of deliberately using a non-asymptotic treatment of the details within the boundary layer, we note that while asymptotic ($Re_\delta \to \infty$) theory predicts an exponentially-small thickness and displacement effect contribution of the inner deck, this is not apparently true at ordinary Reynolds numbers, where many analytic and experimental studies have firmly established that this deck, although indeed very thin, still contributes significantly to the overlying interaction and its displacement thickness growth.[2] Thus we take the point of view here that the inner deck is in fact significant at Reynolds numbers of practical interest. Moreover, it contains all of the skin friction and incipient separation effects in the interaction, which alone are sufficient reasons to examine it in detail. It is further pointed out that application of asymptotic theory results (no matter how rigorous in this limit) to ordinary Reynolds numbers is itself an approximation which may be no more accurate (indeed perhaps less so) than a physically well-constructed non-asymptotic theory. Direct extrapolated-asymptotic versus non-asymptotic theory comparisons definitely show this to be the case for laminar flows (especially as regards the skin friction aspect) and the situation can be even worse in turbulent flow. For example, the asymptotic first order theory formally excludes both the streamwise interactive pressure gradient effect on the shear disturbance deck and both the normal pressure gradient and so-called "streamline divergence" effects on the middle deck; however, physical considerations plus experimental observations and recent comparative numerical studies [2] suggest that these effects are in fact significant at practical Reynolds numbers and should not be neglected. Of course, second order asymptotic corrections can be devised to redress this difficulty but, as Neyfeh and Ragab [3] have shown, run the risk of breaking down even worse when extrapolated to ordinary Reynolds numbers. In the present work, we avoid these problems by using a deliberately nonasymptotic triple-deck model appropriate to realistic Reynolds numbers that includes the inner deck pressure gradient terms plus the middle deck $\partial p/\partial y$ and streamline divergence effects, along with some simplifying approximation that render the resulting theory tractible from an engineering standpoint.

3. TURBULENCE MODELING ACROSS THE INTERACTION

3.1) The Outer Deck Flow

Excluding any freestream turbulence, there is no explicit modeling needed in this upper region of potential inviscid motion; the influence of the turbulent nature of the flow is felt only indirectly through the displacement effect from the underlying decks. The latter is introduced by the physical coupling conditions that both v'/U_{o_e} and p' be continuous with their middle deck counterparts along $y = \delta_o$.

3.2) Turbulence Effects in the Middle Deck

Frozen Turbulence Approximation

Our analysis of this layer rests on the key simplifying assumption that for non-separating interactions the turbulent Reynolds shear stress changes are small and have a negligible back effect on the mean flow properties along the interaction zone; hence this stress can be taken to be "frozen" along each streamline at its appropriate value in the undisturbed incoming boundary layer. This approximation, likewise adopted by a number of earlier investigators with good results, is supported not only by asymptotic analysis but especially by the results of Rose's detailed experimental studies [4] of a non-separating shock turbulent boundary layer interaction which showed that, over the shortranged interaction length straddling the shock, the pressure gradient and inertial forces outside a thin layer near the wall are at least an order of magnitude larger than the corresponding changes in Reynolds stress. Furthermore, there is a substantial body of related experimental results on turbulent boundary layer response to various kinds of sudden perturbations and rapid pressure gradients which also strongly support this view[2]. These studies unanimously confirm that, at least for non-separating flows, significant local Reynolds shear stress disturbances are essentially confined to a thin sublayer within the Law of the Wall region (see below) where the turbulence rapidly adjusts to the local pressure gradient, while outside this region where the Law of the Wake prevails the turbulent stresses respond very slowly and remain nearly frozen at their initial values

far out of the local equilibrium with the wall stress.

Confining attention, then, to the short range local shock interaction zone where the aforementioned "frozen turbulence" approximation is applicable, the disturbance field caused by a weak shock is one of small rotational inviscid perturbation of the incoming non-uniform turbulent boundary layer profile $M_o(y)$ governed by the equations

$$\frac{\partial}{\partial y}\left[\frac{v'(x,y)}{U_o(y)}\right] = \left[\frac{1-M_o^2(y)}{\gamma M_o^2(y)}\right] \cdot \frac{\partial (p'/p_o)}{\partial x} \qquad (1)$$

$$\frac{\partial u'}{\partial x} = -\frac{\partial p'/\partial x}{\rho_o(y)\, U_o(y)} - \frac{dU_o}{dy} \cdot \frac{v'}{U_o} \qquad (2)$$

$$\frac{\partial^2 p'}{\partial y^2} - \frac{2}{M_o}\frac{dM_o}{dy}\frac{\partial p'}{\partial y} + \left[1-M_o^2 - \frac{2u'M_o^2}{U_o}\right]\frac{\partial^2 p'}{\partial x^2} = 0 \qquad (3)$$

as a result of the combined particle-isentropic continuity, x-momentum and energy conservation statements. It is noted that, consistent with the assumed short range character of the interaction, the streamwise variation of the undisturbed turbulent boundary layer properties that would occur over this range are neglected, taking $U_o(y)$, $\rho_o(y)$ and $M_o(y)$ to be arbitrary functions of y only with δ_o, δ_o^* and τ_{w_o} as constants. Note that Eq. (3) is a generalization of Lighthill's well-known pressure perturbation equation for non-uniform flows[5] which includes a non-linear correction term for possible transonic effects within the boundary layer including the diffracted impinging shock above the sonic level of the incoming boundary layer profile. Eqs. (1)-(3) apply to a wide range of incoming boundary layer profiles and provide an account of lateral pressure gradients across the interactive boundary layer.

Incoming Tubulent Boundary Layer Profile

The incoming undisturbed turbulent boundary layer is assumed to be two-dimensional in the x-direction and to possess the classical Law of the Wall/Law of the Wake structure. It is modeled by Walz's[6] composite analytical expression for the resulting velocity profile combined with an adiabatic wall reference temperature method correction for compressibility, allowing arbitrary non-equilibrium values of its shape factor H_i. Thus if we let π be Coles' (incompressible) Wake Function, $\eta \equiv y/\delta_o$ and denote for convenience $R \equiv .41\, Re_{\delta_o^*}/[(1+\pi)(T_w/T_e)^{1+\omega}]$ with $\omega = .76$ and $\gamma = 1.4$ for a perfect gas, then the compressible form of Walz's composite profile may be written:

$$\frac{U_o}{U_e} = 1 + \frac{1}{.41}\sqrt{\frac{C_{f_o}}{2}\left(\frac{T_w}{T_e}\right)}\left[\left(\frac{R}{1+R}\right)\eta^2(1-\eta) - 2\pi + 2\pi\eta^2 \cdot (3-2\eta) + \ln\left(\frac{1+R\eta}{1+R}\right) - (.215+.655R\eta)e^{-3R\eta}\right] \qquad (4)$$

subject to the following condition linking π to C_{f_o} and $Re_{\delta o}{}^*$:

$$2\pi + .215 + \ln(1+R) = .41\sqrt{\frac{C_{f_o}}{2}\left(\frac{T_w}{T_e}\right)} \qquad (5)$$

Eqs. (4) and (5) have the following desirable properties: (a) for $\eta > .10$, U_o/U_e is dominated by a Law of the Wake behavior which correctly satisfies both the outer limit conditions U_o/U_e and $dU_o/dy \to 0$ as $\eta \to 1$; (b) for very small values, U_o assumes a Law of the Wall-type behavior consisting of a logarithmic term that is exponentially damped out into a linear laminar sublayer profile $U/U_e = R\eta$ as $\eta \to 0$; (c) Eq. (4) may be differentiated w.r.t.η to yield an analytical expression for dU_o/dy also, which proves advantageous in solving the middle and inner deck interaction problems. It is evident from these that as $H_{i_I} \to 1$, the outer (wake) part of the profile vanishes leaving essentially a uniform (and inviscid-like) profile except for a very thin sublayer adjacent to the wall.

The defining integral relations for δ_i^* and θ_i^* yields the following relationship that links the wake parameter to the resulting compressible shape factor $H_i = (\delta_i^*/\theta_i^*)$:

$$\frac{H_i - 1}{H_i} = \frac{2}{.41}\sqrt{\left(\frac{T_w}{T_e}\right)\frac{C_{f_o}}{2}}\left(\frac{1 + 1.59\pi + .75\pi^2}{1+\pi}\right) \qquad (6)$$

Equations (4)-(6) provide a very general and accurate model of the profile in terms of three important physical quantities: the shock strength (Ma_1), the displacement thickness Reynolds number $Re_\delta{}^*$, and the Wake function π that reflects the prior upstream history of the incoming boundary layer including possible nonequilibrium pressure gradient and surface mass transfer effects. The resulting relationship of the incompressible shape factor H_i to the Wake Function as a function of Reynolds number for a typical $M_1 = 2.0$ flow is illustrated in Fig. 2. It is seen from this Figure that H_{i_I} approaches a limiting value of unity as $Re_\delta \to \infty$ but that this approach is very gradual, especially for wake function values larger than zero (slightly favorable and adverse pressure gradient upstream flow histories).

With these parameters prescribed, the aforementioned equations may be solved simultaneously for the attendant skin friction C_f, the value of R and, if desired, the H_i appropriate to these flow conditions. Using the adiabatic temperature velocity relationship

$$T_o(y) = T_{w,AD} + \left(Te - T_{w,AD}\right)\frac{U_o^2(y)}{U_{o_e}^2} \qquad (7)$$

the associated Mach number profile $M_o(y) = U_o(\gamma R T_o)^{-\frac{1}{2}}$ and its derivative that are needed for the middle deck interaction solution may then be determined.

3.3) Turbulent Shear Stress Disturbances Along the Inner Deck

This very thin layer lies well within the Law of the Wall region of the incoming turbulent boundary layer profile. The original work of Lighthill[5] treated it by further neglecting the turbulent stresses altogether and considering only the laminar sublayer effect; while this

greatly simplifies the problem and yields an elegant analytical solution, the results can be significantly in error at high Reynolds numbers and cannot explain (and indeed conflict with) the ultimate asymptotic behavior pertaining to the $Re_\delta \to \infty$ limit. The present theory remedies this by extending Lighthill's approach to include the entire Law of the Wall region turbulent stress-effects; the resulting general shear-disturbance sublayer theory provides a non-asymptotic treatment which encompasses the complete range of Reynolds numbers. It is important to note in this connection that our consideration of the entire Law of the Wall combined with the use of the effective inviscid wall concept to treat the inner deck displacement effect eliminates the need for the "blending layer" that is otherwise required to match the disturbance field in the laminar sublayer region with the middle inviscid deck; except for higher order derivative aspects of asymptotic matching, our inner solution effectively includes this blending function since it imposes a boundary condition of vanishing total (laminar plus turbulent) shear disturbance at the outer edge of the deck.

To facilitate a tractible theory, we introduce the following simplifying assumptions. (a) The incoming boundary layer Law of the Wall region is characterized by a constant total (laminar plus turbulent eddy) shear stress and Van Driest-Cebeci type of damped eddy viscosity model. This model is known to be a good one for a wide range of upstream non-separating boundary layer flow histories. (b) For weak incident shock strengths, the sublayer disturbance flow is assumed to be a small perturbation upon the incoming boundary layer; in the resulting linearized disturbance equations, however, all the physically-important effects of streamwise pressure gradient, streamwise and vertical acceleration, and both laminar and turbulent disturbances stresses are retained; (c) For adiabatic flows the undisturbed and perturbation flow Mach numbers are both quite small within the shear disturbance sublayer; consequently, the density perturbations in the sublayer disburbance flow may be neglected while the corresponding modest compressibility effect on the Law of the Wall portion of the undisturbed profile is quite adequately treated by the Eckert reference temperature method wherein incompressible relations are used based on wall recovery temperature properties (this is equivalent in accuracy to, but easier than, the use of Van Driest's compressible Law of the Wall profile [7]). (d) The turbulent fluctuations and the small interactive disturbances are assumed uncorrelated in both the lower and middle decks. (e) The thinness of the inner deck allows the boundary layer-type approximation of neglecting its lateral pressure gradient.

The disturbance field is thus governed by the following continuity and momentum equations:

$$\frac{\partial u'}{\partial x} + \frac{\partial v'}{\partial y} = 0 \tag{8}$$

$$U_o \frac{\partial u'}{\partial x} + v' \frac{dU_o}{dy} + \left(\rho_{w_o}^{-1}\right)\frac{dP'_w}{dx} = \frac{\partial}{\partial y}\left(\nu_{w_o}\frac{\partial u'}{\partial y} + \varepsilon_{T_o}\frac{\partial u'}{\partial y} + \varepsilon_T'\frac{dU_o}{dy}\right) \tag{9}$$

where ρ_{w_o} and ν_{w_o} are evaluated at the adiabatic wall recovery temperature and where it should be noted that the kinematic eddy viscosity perturbation ε_T' is being taken into account. The corresponding undisturbed turbulent boundary layer Law of the Wall profile $U_o(y)$ is governed by

$$\tau_o(y) = \text{const.} = \tau_{w_o} = \left[\mu_{w_o} + \rho_{w_o}\varepsilon_{T_o}(y)\right]\frac{dU_o}{dy} \tag{10}$$

where according to the Van Driest-Cebeci eddy viscosity model with $y^+ = \left(y\sqrt{\tau_{w_o}/\rho_{w_o}}\right)/\nu_{w_o}$

$$\varepsilon_{T_o} = \left[.41\nu\left(1-e^{-y^+/A}\right)\right]^2\frac{\partial u}{\partial y} \tag{11}$$

which yields for non-separating flow disturbances that

$$\varepsilon_{T_o} = \left[.41\gamma\left(1-e^{-y^+/A}\right)\right]^2\frac{dU_o}{dy} \tag{12}$$

$$\varepsilon_T' = \left(\frac{\partial u'/\partial y}{dU_o/dy}\right)\varepsilon_{T_o} \tag{13}$$

Here, A is the so-called Van Driest damping "constant;" we use the commonly-accepted value A = 26 although it is understood that a larger value may improve the experimental agreement in regions of shock-boundary layer interaction. Substituting (13) into (9) we thus have the disturbance momentum equation

$$U_o\frac{\partial u'}{\partial x} + v'\frac{dU_o}{dy} + \left(\rho_{w_o}^{-1}\right)\frac{\partial p'_w}{\partial x} = \frac{\partial}{\partial y}\left[\left(\nu_{w_o} + 2\cdot\varepsilon_{T_o}\right)\frac{\partial u'}{\partial y}\right] \tag{14}$$

from which we have seen that inclusion of the eddy viscosity perturbation has exactly doubled the turbulent shear stress disturbance term.

We solve these Equations subject to the wall boundary conditions $U_o(0) = u(x,o) = v(x,o) = 0$ plus an initial condition $u(-\infty,y) = 0$ requiring that all interactive disturbances vanish far upstream of the impinging shock. Futhermore, at some distance δ_{3L} sufficiently far from the wall, u' must pass over to the inviscid solution u'_{inv} along the bottom of the middle deck, as governed by

$$U_o\frac{\partial U_{inv}}{\partial x} = v'_{inv}\frac{dU_o}{dy} + \left(\rho_{w_o}\right)^{-1}\frac{dP_w}{dx} = 0 \tag{15}$$

with δ_{3L} defined as the height where the total shear disturbance (proportional to $\partial u'/\partial y$) of the inner solution vanishes to a desired accuracy.

4. SOLUTION METHODOLOGY AND RESULTS

The solution to the foregoing triple deck problem is achieved for small linearized disturbances ahead of, behind and below the local shock jump, which gives reasonably accurate predictions for all the properties of engineering interest. The resulting equations can be solved by a Fourier transform method to yield the viscous interaction field physics for non-

separating flows including the upstream influence, the lateral pressure gradient near the shock and the onset of incipient separation (see Refs. 2 and 12 for the details of this solution). Numerous detailed comparisons with experiment[9] have shown that it gives a good account of all the important features of the interaction over a wide range of Mach-Reynolds number conditions.

4.1) Fourier Transformation Method

We only briefly outline here the steps involved, since full details can be found elsewhere. Following Fourier Transformation w.r.t.x , the resulting middle deck pressure problem from Eq. 3 is an ordinary differential equation in y that can be solved numerically quite efficiently for the input turbulent boundary layer profile Mo(y) of Section 3.2. In particular, for the upstream interactive pressure rise we find from the appropriate Fourier inversion process using the calculus of residues that

$$p_w' = \Delta p \, e^{x/\ell_u} \tag{16}$$

where ΔP is the overall shock pressure jump while ℓ_u is the characteristic upstream distance given by

$$\ell_u = \frac{M_{e_1}^2 \, I_o}{\sqrt{M_{e_1}^2 - 1}} + \frac{\sqrt{M_{e_1}^2 - 1}\, I_1}{M_{e_1}^2} \tag{17a}$$

in terms of the following profile-dependent integrals evaluated by the aforementioned turbulent Law of the Wall/Law of the Wake model:

$$I_o \equiv \int_{y_{weff}}^{\delta_o} \left| \left[1 - M_o^2(z) \right] \Big/ M_o^2(z) \right| dz \tag{17b}$$

$$I_1 \equiv \int_o^{\delta_o} M_{on}^2(z)\, dz \tag{17c}$$

The parameter y_{weff} here is the effective inviscid wall shift given by the displacement thickness of the underlying inner deck.

The corresponding Fourier transformation of the inner deck problem of Section 3.3, followed by the introduction of new inner deck variables and y-scaling defined by Inger[2], yields a set of ordinary differential equation boundary value problems in a "universal" form that can be solved and tabulated once and for all. An example of this is illustrated in Fig. 3, which shows the resulting inner deck streamwise velocity profiles in terms of the eddy viscosity effect as expressed by the authors' Interactive Turbulence Parameter[2]

$$T \equiv (.41)^2 \frac{\rho_{o_w} \tau_{w_o}}{\mu_{o_w}^2} \left(\frac{\mu_{o_w}^2 \ell_u}{\rho_{o_w} \tau_{w_o}} \right)^{2/3} \tag{18}$$

The typical Reynolds number and wake function-dependence of this parameter is illustrated in Figure 4, where it is seen that it grows to large values with increasing Re_δ , as well as increasing with π .

We further obtain the following result for the deck's displacement thickness:

$$y_{weff} = .776 \left(\frac{\mu_{o_w}^2 \ell_u}{\rho_{o_w} \tau_{w_o}} \right)^{1/3} H(T) \tag{19}$$

where the eddy viscosity effect-function H(T) is given in Figure 5. The simultaneous solution of Eqs. (17)-(19) for ℓ_u and y_{weff} implements the matching of the inner and middle decks. The resulting values of the inner deck height expressed as a fraction of the incoming undisturbed boundary layer thickness are plotted versus Reynolds number with π as a parameter in Figure 6; also shown for comparison are the corresponding sonic height ratio values. It is clearly seen how rapidly y_{weff}/δ_o decreases with increasing Re_δ , reaching exceedingly small values indeed, relative to the much more gradual decrease in y_{sonic}/δ_o. It is also interesting to note here, as one would expect on physical grounds, that while the inner deck thickness is hardly affected by π, the sonic height (which lies within the wake region) is significantly influenced and increases with the value of the Wake function.

Finally, we note the companion result for the upstream skin friction that

$$\tau_w' = -1.372 \, p_w'(x) f_p(x) \left[\frac{\rho_{w_o}^2 \ell_u \tau_{w_o}}{\mu^2 w_o} \right]^{-1/3} S(T) \tag{20a}$$

where

$$f_{p(x)} \equiv \frac{2}{3} \left[\frac{\ell_u (p_w')^{3/2}}{\int_{-\infty}^{x} (p_w')^{3/2} dx} \right]^{2/3} \tag{20b}$$

and S(T) is another interactive-turbulence effect function, also plotted in Figure 5.

Figure 5 is a central result of the present general turbulent shear-disturbance inner deck treatment; it gives a unified account of the inner interactive physics over the entire Reynolds number range from quasi-laminar behavior at $T \ll 1$ (lower Reynolds numbers) to the opposite extreme of wall turbulence-dominated behavior at $T \gg 1$ pertaining to asymptotic theory at very large Reynolds numbers where the inner deck thickness and its disturbance field become vanishingly small.

4.2) Predictive Results Showing the Role of the Turbulence Modeling Parameters

A computer program has been constructed to carry out the foregoing solution method; it involves the middle-deck disturbance pressure solution coupled to the inner deck by means of the effective wall shift combined with an upstream influence solution subroutine (the corresponding local total interactive displacement thickness growth and skin friction are also obtained). This provides a very general fundamental description of the boundary layer in terms of three arbitrary parameters: preshock Mach number, boundary layer displacement thickness Reynolds number, and either the wake function or the incompressible shape factor Hi_1.

Based on the aforementioned program, an extensive parametric study has been carried

out to show the sensitivity of predicted interaction zone properties to the various key turbulent flow modeling parameters. For example, Figure 7 shows for a typical $M_1 = 2.0$ interaction the effect of the Wake Function on the interactive upstream influence distance ℓu (in ratio to the undisturbed boundary layer thickness δ_o) as a function of Reynolds number. Clearly, the effect is an important one over a wide range of Reynolds numbers, indicating a significant increase in $\ell u/\delta o$ with π, and suggests that accounting for the upstream boundary layer history can be important in the experimental validation of CFD predictions of such interactions. In this connection, it should be noted that this wake function aspect is totally lost in the leading approximation of the asymptotic triple deck approach (which is based on the limiting value $Hi_1 = 1.0$ pertaining to the infinite Reynolds number limit, wherein the wake component completely vanishes).

Another interesting aspect of the turbulence modeling is the eddy viscosity perturbation effect in the inner deck; this is illustrated in Figure 8, where we show how the predicted upstream influence distance is altered by including (or neglecting) this effect. At moderately-high Reynolds numbers ($Re_\delta \leq 10^6$), the effect is seen to be quite large, such that neglect of the interactive disturbance to ϵ_T can consequently underpredict ℓu by hundreds of percent. On the other hand, at very large Re where the interactive flow is essentially inviscid-dominated and influenced only by the outer wake region of the incoming boundary layer, the eddy viscosity perturbations have only a small effect. Figure 8 also serves to reemphasize the fact that the present theory applies to a very wide range of practical Reynolds numbers.

In Figure 9, we conclude by illustrating the excellent agreement of the present predictions of $\ell u/\delta o$ with experiment when one properly accounts for the important effect of the incoming boundary layer shape factor (or wake function). Clearly, the experimental validation of any theoretical prediction will require a rather careful determination of the wake component aspects of the incoming turbulent boundary layer.

REFERENCES

1. Marvin, J. G., "Turbulence Modeling for Computational Aerodynamics," AIAA Paper 82-0164, 1982.

2. Inger, G.R., "Upstream Influence and Skin Friction in Non-Separating Shock Turbulent Boundary Layer Interactions," AIAA Paper No. 80-1411, Snowmass, Colorado, July 1980. See also "Nonasymptotic Theory of Unseparated Turbulent Boundary Layer Interaction," in Numerical and Physical Aspects of Aerodynamic Flows (T. Cebeci, Ed.), Springer-Verlag, N.Y. 1983.

3. Ragab, S.A., and Nayfeh, A.H., "A Second Order Asymptotic Solution for Laminar Separation of Supersonic Flows Past Compression Ramps," AIAA Paper 78-1132, 1978.

4. Rose, W.C., and Childs, M.E., "Reynolds Shear Stress Measurements in a Compressible Boundary Layer Within a Shock Wave-Induced Adverse Pressure Gradient," JFM 65, 1, 1974, pp. 177-188.

5. Lighthill, M.J., "On Boundary Layers and Upstream Influence; II. Supersonic Flow Without Separation," Proc. Royal Soc. A 217, 1953, pp. 578-587.

6. Walz, A., Boundary Layers of Flow and Temperature, M.I.T. Press, 1969, pp. 113-116.

7. Van Driest, E.R., "Turbulent Boundary Layers in Compressible Fluid," Journal of Aeronaut. Sci. 18, March 1951, pp. 145-60.

8. Inger, G.R., "The Modular Application of a Shock/Boundary Layer Interaction Solution to Supercritical Viscous Inviscid Flor Field Analysis," in Computational Methods in Viscous Flows 3, Pineridge Press, U.K., 1984, pp. 475-512.

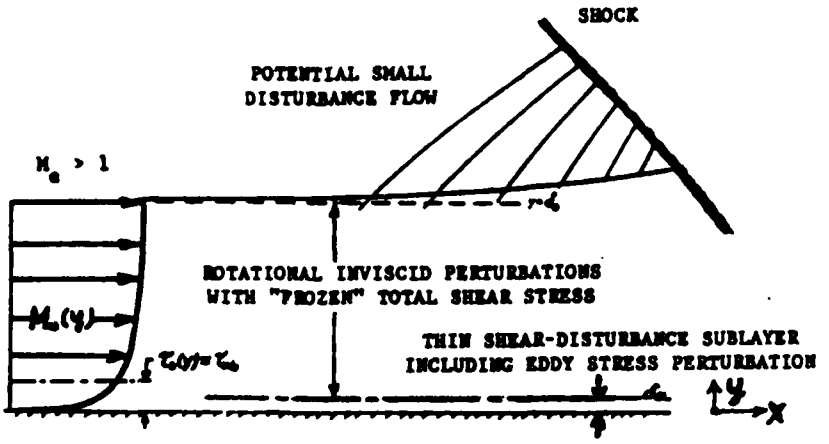

Fig. 1. Triple-Deck Structure of the Interaction Zone

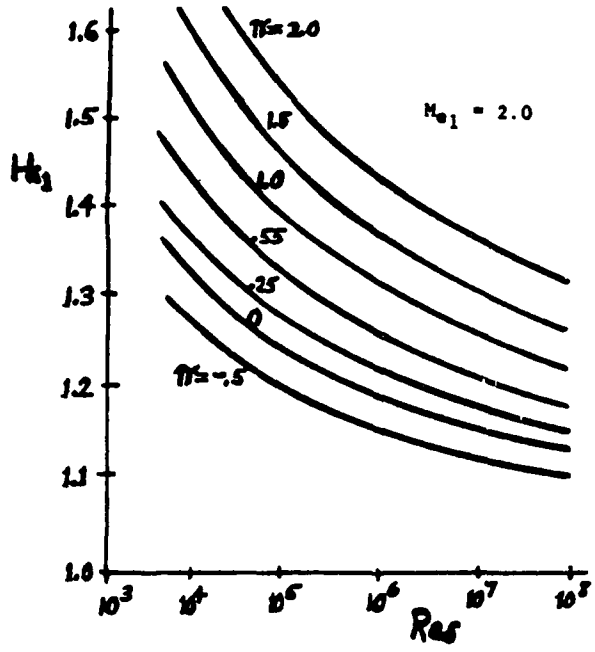

Fig. 2. Incompressible Shape Factor vs. Reynolds Number with the Wake Function as a Parameter

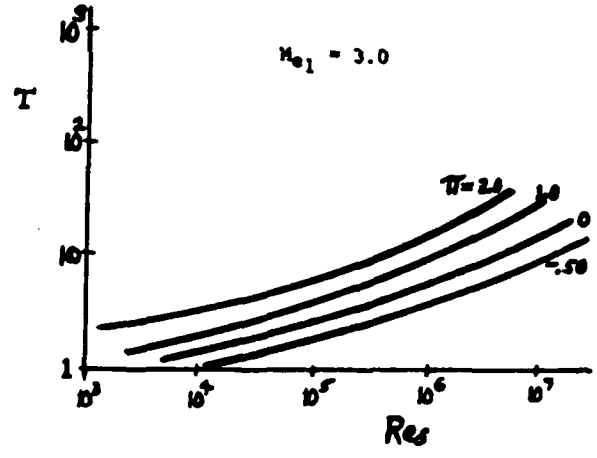

Fig. 4. Variation of the Interactive Turbulence Parameter with Reynolds Number for Various Wake Function Values

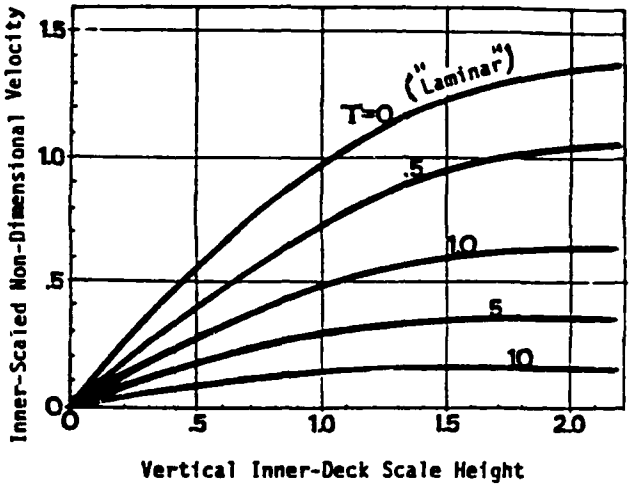

Fig. 3. Streamwise Disturbance Velocity Profiles Across the Inner Deck for Various Values of the Interactive Turbulence Parameter

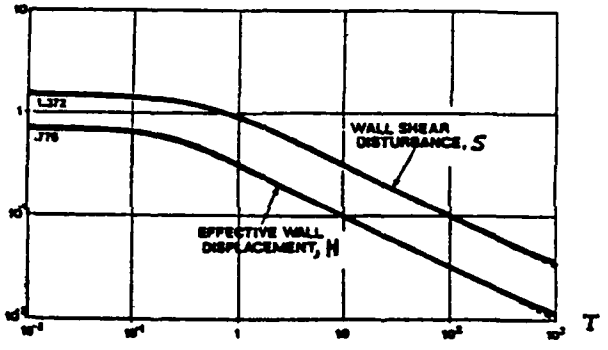

Fig. 5. Turbulent Interaction Parameter Effect on Interactive Displace-Thickness and Skin Friction Functions

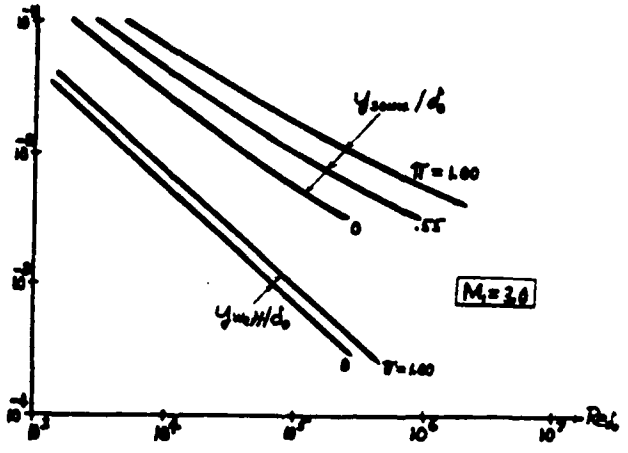

Fig. 6. Non-Dimensionalized Inner Deck Thickness and Sonic Height Variations with Reynolds Number with the Wake Function as a Parameter

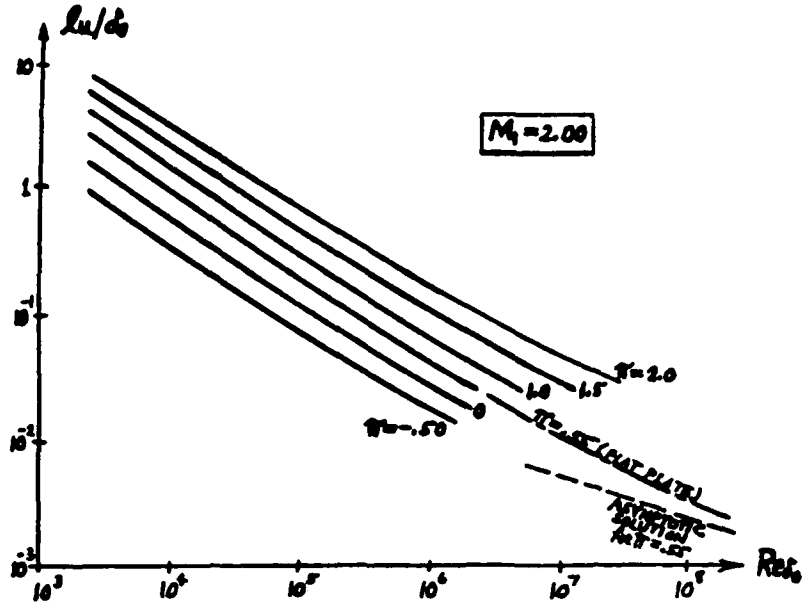

FIG. 7

Predicted Wake Factor Effect on the Upstream Influence of Non-Separating Shock-Turbulent Layer Interactions at Mach Two

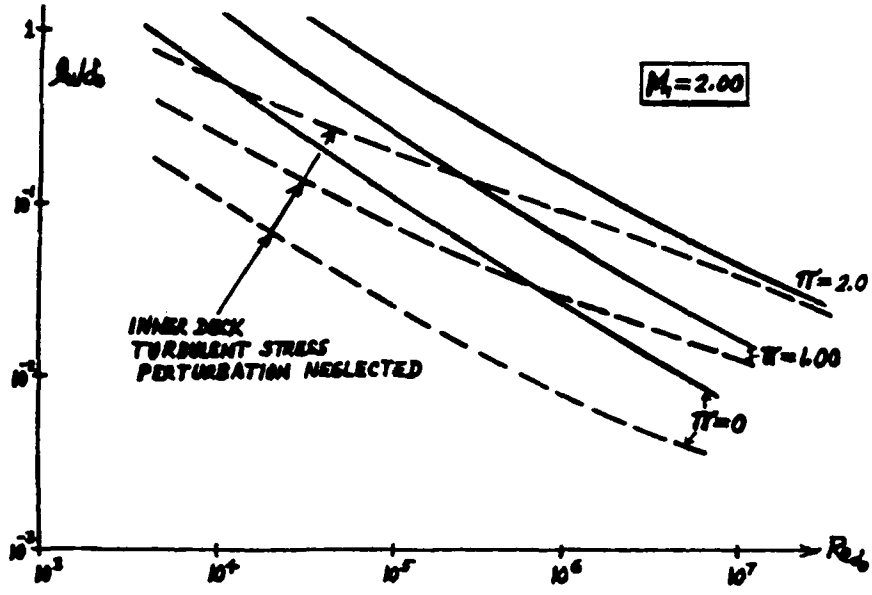

FIG. 8

Typical Effect of the Turbulent Eddy Viscosity Disturbance in the Inner Law of the Wall Region on Upstream Influence Predictions

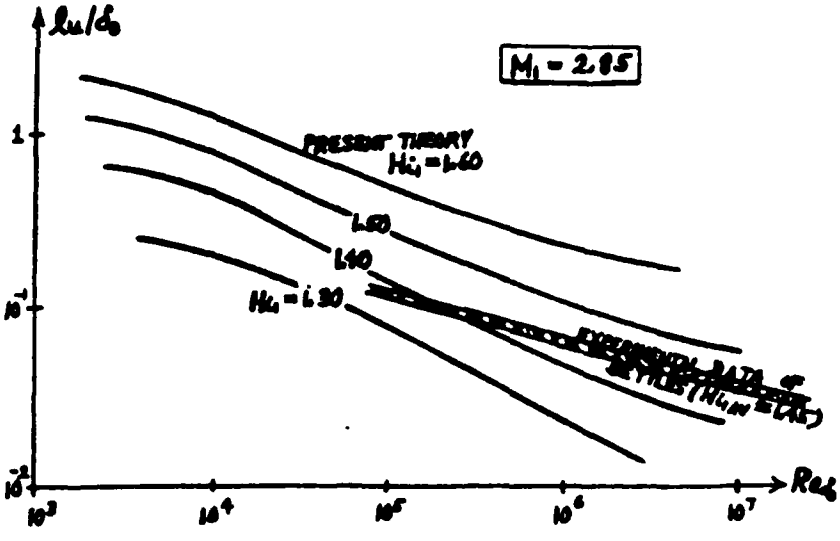

FIG. 9

Typical Shape Factor Effect on the Experimental Validation of Predicted Upstream Influence vs. Reynolds Number (Weak Compression Corners).

APPENDIX D

MEETING OF THE WORKING GROUP

ON 3-D SHOCK WAVE/

TURBULENT BOUNDARY LAYER INTERACTIONS

JULY 11-12, 1988

PRINCETON UNIVERSITY

COPIES OF PRESENTED MATERIAL

SUMMARY

RESEARCH NEEDS IN 3-D SHOCK-WAVE/ TURBULENT BOUNDARY LAYERS INTERACTIONS

After considerable discussion, thirteen separate topics were identified as requiring immediate research attention. They are (in no particular order);as

1. Analytical treatments of near-wall boundary layer behavior to develop efficient wall-functions for computation.

2. Experimental (and computational) studies to determine the effect of modifying the upstream boundary layer using pressure gradients, blowing and roughness.

3. Measurements of skin friction and heat transfer distributions.

4. Studies to identify where turbulence models are important for the accuracy of the computations (in large regions of the interaction, turbulence may not be playing a significant role).

5. Extension of calculations and experiments to higher Mach numbers (> 6).

6. Extension of calculations and experiments to more complex interactions (for example, shock/shock interactions, interactions with floor and sidewall boundary layers, more complicated shock-generator geometry).

7. More detailed flowfield investigations for carefully selected interactions. These measurements should have enough detail to give the flowfield structure, unsteady characteristics, turbulence behavior, skin friction and heat transfer distributions.

8. Studies of the downstream boundary layer relaxation (very important for inlet design).

9. Alteration and control applied within the interaction zone using, for example, bleeding, blowing, flow guides.

10. Exploratory calculation of non-adiabatic interactions.

11. Full characterization of incoming flow conditions, including freestream turbulence, spanwise inhomogeneities (3-D effects in nominally 2-D flows), changes in boundary layer turbulence due to Mach number effects (especially $M > 6$).